Supporting Information for: Methionine adenosyltransferase engineering to enable bioorthogonal platforms for AdoMet-utilizing enzymes

Tyler D. Huber[1,2], Jonathan Clinger[3], Yang Liu[1,2], Weijun Xu[3], Mitchell D. Miller[3], George N. Phillips, Jr.[3,4], and Jon S. Thorson[1,2]

[1]Department of Pharmaceutical Sciences, College of Pharmacy, University of Kentucky, 789 South Limestone Street, Lexington, KY 40536-0596, USA; [2]Center for Pharmaceutical Research and Innovation (CPRI), College of Pharmacy, University of Kentucky, 789 South Limestone Street, Lexington, KY 40536-0596, USA; [3]Department of Biosciences, Rice University, 6100 Main Street, Houston, TX 77251-1892, USA; [4]Department of Chemistry, Rice University, Space Science 201, Houston, TX 77251-1892, USA

Table of Contents

1. General materials and methods.

1.1 General materials. Unless otherwise stated, all general chemicals and reagents (including methionine analogues **2**, **3**, and **13** – **15**) were purchased from Sigma-Aldrich (St. Louis, MO) and were reagent grade or better. Metamine, or (2*S*)-4-(methylsulfanyl)butane-1,2-diamine, was purchased from Enamine Ltd. (Kyiv, Ukraine). Metamide, or (*S*)-2-amino-4-(methylthio)butanamide, was synthesized as previously described.[S1] *S*-adenosyl-L-methionine (AdoMet) was purchased as a 32 mM solution in 10% EtOH/5 mM H_2SO_4 from New England Biolabs (Ipswich, MA). *E. coli* BL21(DE3) competent cells were purchased from New England Biolabs (Ipswich, MA). The pET28a *E. coli* expression vector was purchased from Novagen (Madison, WI). Primers were purchased from Integrated DNA Technologies (Coralville, IA). QuikChange II site-directed mutagenesis kits were purchased from Agilent Technologies (Santa Clara, CA). PD-10 columns and Ni-NTA superflow columns were purchased from GE Healthcare (Piscataway, NJ). Crystal screen kits were purchased from Hampton Research (Aliso Viejo, CA), Molecular Dimensions (Altamonte Springs, FL), Rigaku (Seattle, WA) and Microlytic (Burlington, MA).

1.2 General methods. X-ray data were collected at beamline 21-ID-F (LS-CAT) in the Advanced Photon Source at Argonne National Laboratory (Chicago, IL). NMR spectra were obtained on a Varian Unity Inova 400 MHz instrument (Palo Alto, CA) at the University of Kentucky College of Pharmacy NMR facility using $CDCl_3$ (D, 99.96%) with or without 0.05% v/v TMS from Cambridge Isotopes (Cambridge Isotope Laboratories, MA). ^1H and ^{13}C chemical shifts were referenced to internal solvent resonances. Multiplicities are indicated by s (singlet), d (doublet), dd (doublet of doublets), t (triplet), q (quartet), quin (quintet), m (multiplet), and br (broad). Chemical shifts are reported in parts per million (ppm) and coupling constants *J* are given in Hz. Routine ^{13}C NMR spectra were fully decoupled by broad-broad WALTZ decoupling. All NMR spectra were recorded at ambient temperature.

Normal-phase flash chromatography was performed on 40–63 µm, 60 Å silica gel (Silicycle, Quebec). Analytical TLC was performed on silica gel glass TLC plates (EMD Chemicals Inc, Gibbstown, NJ). Visualization was accomplished with UV light (254 nm) followed by staining with dilute H_2SO_4 (5% in EtOH) solution, $KMnO_4$ solution (1.5 g of $KMnO_4$, 10g K_2CO_3, and 1.25 mL 10% NaOH in 200 mL water) and heating, or 10% ninhydrin in EtOH and heating. HPLC was accomplished using an Agilent 1260 system equipped with a DAD detector. **HPLC Method:** To monitor enzyme reactions, analytical reverse-phase (RP) HPLC was conducted with a Luna C_{18} (5 µm, 4.6 mm × 250 mm; Phenomenex, Torrance, California, USA) column [gradient of 1% B to 20% B over 5 min, 20% B to 55% B over 15 min, 55% B to 100% B over 1 min, 100% B for 5 min, 100% B to 1% B over 1 min, 1% B for 8 min (A = ddH_2O with 0.1% formic acid; B = acetonitrile) flow rate = 0.4 mL min^{-1}; A_{254}, A_{260}].

2. General procedure for the synthesis of metOMe, metOEt, metOPr, and metOBu

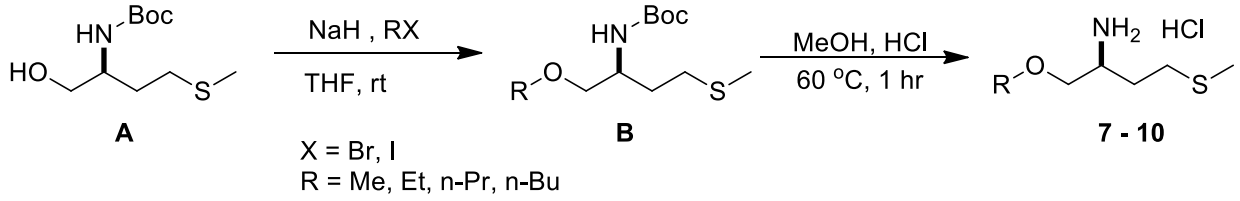

Rxn 1: NaH (26 mg, 0.65 mmol) was added to a solution of compound **A** (0.7 equivalents) in 4.3 mL dry THF at 0 °C. The mixture was stirred for 10 min, alkyl halide (1.3 equivalents) was added, and the reaction continued for an additional 1.5 hr with stirring (monitored by TLC and LC-MS). The organics were removed under vacuum and the residue was purified by normal-phase column chromatography (*n*-hexane:EtOAc, 20:1 ~ 8:1) to give the desired product **B**.

Rxn 2: Compound **B** (0.2 mmol) was dissolved in 1.5 mL MeOH. 0.5 mL concentrated HCl was added and the mixture was refluxed at 60 °C for 1.5 hr (monitored by TLC, stained by iodine). Upon completion, solvent was removed under vacuum to give the HCl salt of product **7**, **8**, **9**, or **10**.

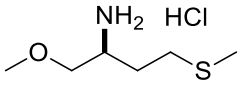

(*S*)-1-Methoxy-4-(methylthio)butan-2-amine (metOMe, 7). Methyl iodide (122 mg, 0.86 mmol) was used to obtain the product as a white solid (66 mg, 2 steps, 81% yield). ^{1}H NMR (400 MHz, $CDCl_3$) δ: 8.49 (s, 2H), 3.53-3.69 (m, 3H), 3.42 (s, 3H), 2.62-2.75 (m, 2H) 2.14-2.26 (m, 1H), 2.12 (s, 3H), 1.92-2.05 (m, 1H). ^{13}C NMR (100 MHz, $CDCl_3$) δ: 71.2, 59.2, 50.6, 29.8, 28.5, 15.2. HRMS $[M+H]^+$ calculated for $C_6H_{16}NOS$ 150.0947, found 150.0946.

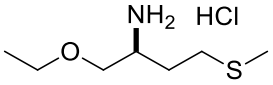

(*S*)-1-Ethoxy-4-(methylthio)butan-2-amine (metOEt, 8). Ethyl iodide (135 mg, 0.86 mmol) was used to obtain the product as a white solid (38 mg, 2 steps, 55% yield). ^{1}H NMR (400 MHz, $CDCl_3$) δ: 8.47 (s, 2H), 3.49-3.73 (m, 5H), 2.60-2.75 (m, 2H) 2.14-2.25 (m, 1H), 2.12 (s, 3H), 1.94-2.05 (m, 1H), 1.24 (t, J = 7.0 Hz 3H). ^{13}C NMR (100 MHz, $CDCl_3$) δ: 69.0, 67.0, 50.8, 29.8, 28.5, 15.1, 15.0. HRMS $[M+H]^+$ calculated for $C_7H_{18}NOS$ 164.1104, found 164.1101.

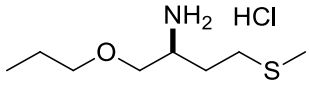

(*S*)-4-(Methylthio)-1-propoxybutan-2-amine (metOPr, 9). 1-Bromopropane (105 mg, 0.86 mmol) was used to obtain the product as a light yellow solid (115 mg, 2 steps, 49% yield). ^{1}H NMR (400 MHz, $CDCl_3$) δ: 8.48 (s, 2H), 3.52-3.71 (m, 3H), 3.40-3.51 (m, 2H), 2.61-2.76 (m, 2H) 2.14-2.25 (m, 1H), 2.12 (s, 3H), 1.94-2.05 (m, 1H), 1.57-1.68 (m, 2H), 0.92 (t, J = 7.5 Hz 3H). ^{13}C NMR (100 MHz, $CDCl_3$) δ: 73.3, 69.2, 50.7, 29.8, 28.5, 22.6, 15.1, 10.5. HRMS $[M+H]^+$ calculated for $C_8H_{20}NOS$ 178.1260, found 178.1255.

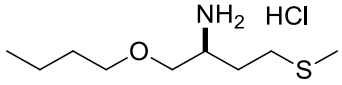

(*S*)-1-Butoxy-4-(methylthio)butan-2-amine (metOBu, 10). *n*-Butyl bromide (118 mg, 0.86 mmol) was used to obtain the product as a light yellow solid (251 mg, 2 steps, 55% yield). ^{1}H NMR (400 MHz, $CDCl_3$) δ: 8.45 (s, 2H), 3.55-3.71 (m, 3H), 3.46-3.53 (m, 2H), 2.62-2.77 (m, 2H) 2.15-2.25 (m, 1H), 2.13 (s, 3H), 1.94-2.07 (m, 1H), 1.54-1.64 (m, 2H), 1.31-1.42 (m, 2H), 0.92 (t, J = 7.5 Hz 3H). ^{13}C NMR (100 MHz, $CDCl_3$) δ: 71.5, 69.2, 50.8, 31.4, 29.8, 28.5, 19.2, 15.1, 13.9. HRMS $[M+H]^+$ calculated for $C_9H_{22}NOS$ 192.1417, found 192.1416.

3. General procedure for the synthesis of metolMe, metolEt, and metolPr

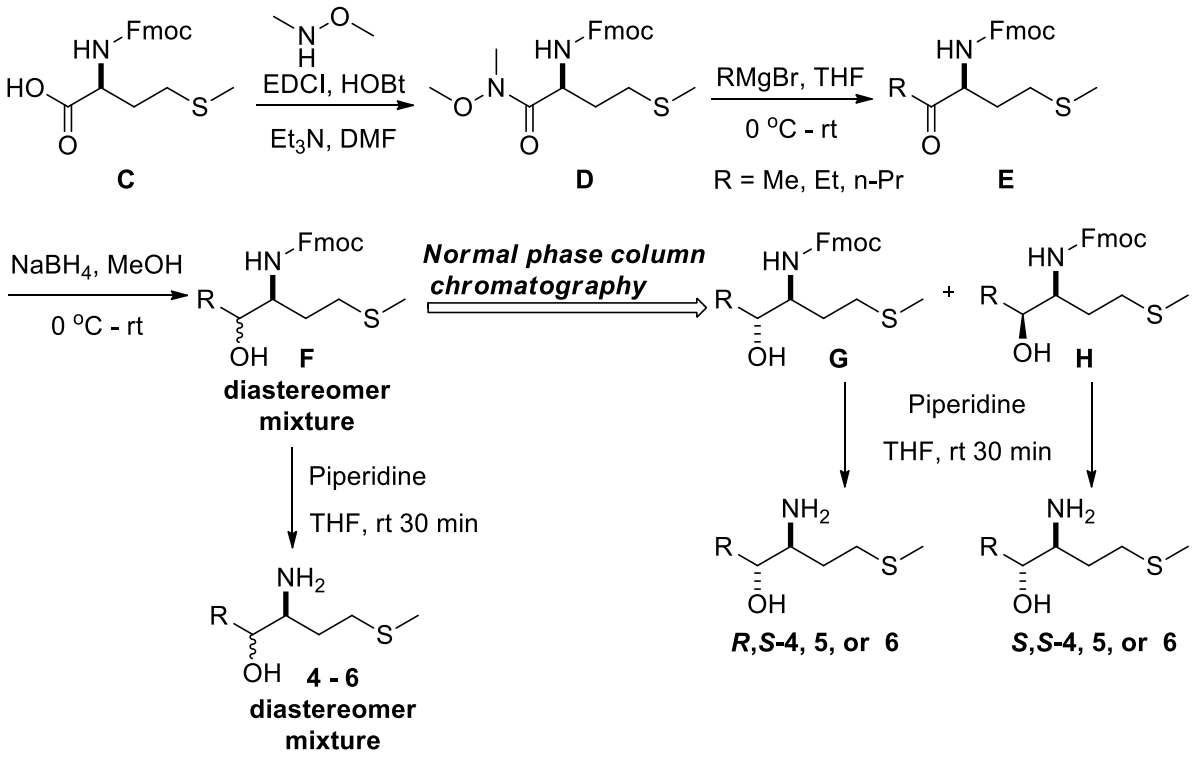

Rxn 1: *N*,*O*-dimethylhydroxylamine hydrochloride (1.25 g, 12.5 mmol), HOBt (1.7 g, 12.5 mmol) and EDCl (2.4 g, 12.5 mmol) were added to a solution of compound **C** (3.7 g, 10 mmol) in 25 mL dry DMF. The mixture was stirred for 1 hr, then Et_3N (1.7 mL, 12.5 mmol) was added and the reaction stirred for an additional 5 hr (monitored by TLC and LC-MS). Upon completion, the reaction was diluted with 100 mL H_2O and extracted with EtOAc (50 mL x 2), washed with water (100 mL x 2), brine (50 mL x1) and then dried over Na_2SO_4. The mixture was filtered, organic solvent was removed under vacuum, and the crude mixture purified by normal-phase column chromatography (*n*-hexane:EtOAc, 4:1 ~ 1:1) to give the desired product **D** as a white solid, 75% yield.

Rxn 2: Alkyl magnesium halide (3 M in THF, 3.0 mmol, 1 mL total volume) was added dropwise to a solution of **D** (1.0 g, 2.4 mmol) in 20 mL dry THF at 0 °C and the mixture was stirred at room temperature for 6 hr (monitored by TLC and LC-MS). Saturated NH_4Cl solution (50 mL) was added to quench the reaction and the reaction was extracted by EtOAc (50 mL x 2), washed with water (50 mL x 2), brine (50 mL x 1) and dried over Na_2SO_4. The organic solvent was removed under vacuum and the residue was purified by normal-phase column chromatography (*n*-hexane:EtOAc, 8:1 ~ 2:1) to give the desired product **E** (R = Me, 69% yield; R = Et, 60% yield; R = *n*-Pr, 51% yield).

Rxn 3: $NaBH_4$ (74 mg, 2.0 mmol) was added to a solution of **E** (1.0 mmol) in 5 mL of MeOH at 0 °C and the mixture was stirred at room temperature for 8 hr (monitored by TLC and LC-MS). The reaction was quenched with the addition of 30 mL H_2O and the mixture was extracted by EtOAc (30 mL x 2), washed with water (30 mL x 2), brine (30 mL x 1) and then dried over Na_2SO_4. The organics were removed under vacuum and the residue was purified by normal-phase column chromatography (*n*-hexane:EtOAc, 8:1 ~ 2:1) to give the desired product **F** (R = Me, 75% yield; R = Et, 66% yield; R = *n*-Pr, 71% yield).

Rxn 4: Piperidine (1 mL, 12.5 mmol) was added to a solution of **F** (0.26 mmol) in 4 mL THF and the mixture was stirred for 30 min (monitored by TLC). Upon completion, solvent was removed under vacuum and the residue was purified by normal-phase column chromatography (CH_2Cl_2:MeOH, 10:1 ~ 4:1) to give the desired product **4, 5, or 6**.

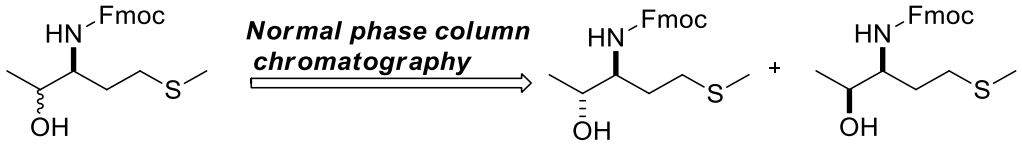

N-Fmoc-**4** *N*-Fmoc-*R*,*S*-**4** *N*-Fmoc-*S*,*S*-**4**

(9*H*-Fluoren-9-yl)methyl [(3*S*)-4-hydroxy-1-(methylthio)pentan-3-yl]carbamate (*N*-Fmoc-4, *N*-Fmoc-*R*,*S*-4, and *N*-Fmoc-*S*,*S*-4). Methyl magnesium bromide (3 M in THF), (1mL, 3mmol) was used to obtain the diastereomeric mixture (*N*-Fmoc-**4**) as a white solid (280 mg, 3 steps, 32% yield), which was resolved by normal-phase column chromatography to obtain *N*-Fmoc-***R*,*S*-4** (31 mg, 3 steps, 3.5 % yield) and *N*-Fmoc-***S*,*S*-4** (95 mg, 3 steps, 10.8% yield). Enantioselectivity was determined by the NMR analysis of (*R*) and (*S*) Mosher esters, *N*-Fmoc-***S*,*S*-4-(*R*)-MTPA** and *N*-Fmoc-***S*,*S*-4-(*S*)-MTPA,** obtained from *N*-Fmoc-***S*,*S*-4** (see below) following standard protocols.[S2]

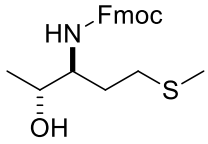

(9*H*-Fluoren-9-yl)methyl [(3*S*,4*R*)-4-hydroxy-1-(methylthio)pentan-3-yl]carbamate (*N*-Fmoc-*R*,*S*-4). ^{1}H NMR (400 MHz, $CDCl_3$) δ: 7.75 (d, *J* = 7.4 Hz 2H), 7.58 (d, *J* = 7.4 Hz 2H), 7.38 (t, *J* = 7.4 Hz 2H), 7.30 (t, *J* = 7.4 Hz 2H), 4.98 (d, *J* = 9.4 Hz 1H), 4.44 (d, *J* = 6.7 Hz 2H), 4.20 (t, *J* = 6.7 Hz 1H), 3.80-3.88 (m, 1H), 3.55-3.65 (m, 1H), 2.49 (s, 2H), 2.08 (s, 3H), 1.75-1.85 (m, 2H), 1.16 (d, *J* = 6.3 Hz 3H). HRMS [M+H]$^+$ calculated for $C_{21}H_{26}NO_3S$ 372.1628, found 372.1625.

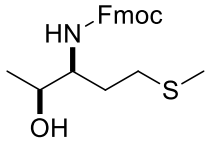

(9*H*-Fluoren-9-yl)methyl [(3*S*,4*S*)-4-hydroxy-1-(methylthio)pentan-3-yl]carbamate (*N*-Fmoc-*S*,*S*-4). ^{1}H NMR (400 MHz, $CDCl_3$) δ: 7.75 (d, *J* = 7.4 Hz 2H), 7.58 (d, *J* = 7.4 Hz 2H), 7.38 (t, *J* = 7.4 Hz 2H), 7.30 (t, *J* = 7.4 Hz 2H), 4.98 (d, *J* = 9.4 Hz 1H), 4.44 (d, *J* = 6.7 Hz 2H), 4.20 (t, *J* = 6.7 Hz 1H), 3.80-3.88 (m, 1H), 3.55-3.65 (m, 1H), 2.49 (s, 2H), 2.08 (s, 3H), 1.75-1.85 (m, 2H), 1.16 (d, *J* = 6.3 Hz 3H). HRMS [M+H]$^+$ calculated for $C_{21}H_{26}NO_3S$ 372.1628, found 372.1629.

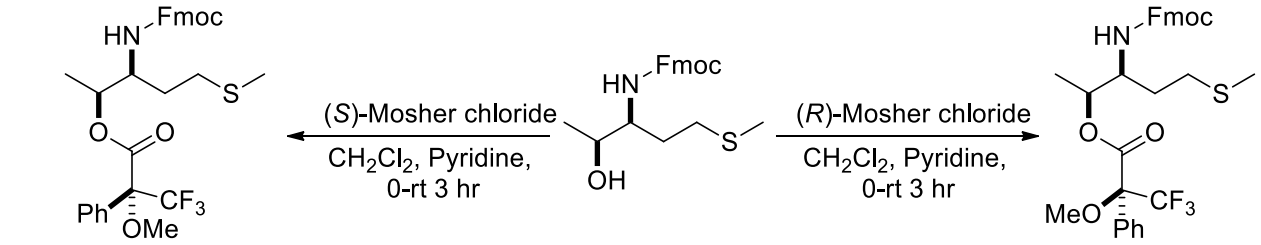

N-Fmoc-*S*,*S*-**4**-(*R*)-MTPA *N*-Fmoc-*S*,*S*-**4** *N*-Fmoc-*S*,*S*-**4**-(*S*)-MTPA

N*-Fmoc-*S*,*S*-4-(*R*)-MTPA.** The procedures applied to the synthesis of *N*-Fmoc-S*,*S*-4-(*R*)-MTPA** used *N*-Fmoc-***S*,*S*-4** (10 mg, 0.027 mmol), pyridine (10 µL, 0.1 mmol) and (*S*)-Mosher chloride (20 µL, 0.1 mmol) to obtain the product as a white solid (12 mg, 89% yield). ^{1}H NMR (400 MHz, $CDCl_3$) δ: 7.77 (d, *J* = 7.4 Hz 2H), 7.57 (d, *J* = 7.4 Hz 2H), 7.28 -7.50 (m, 9H), 5.09-5.17 (m, 1H), 4.58 (d, *J* = 9.4 Hz 1H), 4.48 (d, *J* = 6.3 Hz 2H), 4.20 (t, *J* = 6.3 Hz 1H), 3.90 (t, *J* = 10.1 Hz 1H), 3.45 (s, 3H), 2.31-2.52 (m, 2H), 2.04 (s, 3H), 1.78-1.90 (m, 1H), 1.45-1.55 (m, 1H), 1.28 (d, *J* = 6.7 Hz 3H). HRMS $[M+H]^+$ calculated for $C_{31}H_{33}F_3NO_5S$ 588.2026, found 588.2023.

N*-Fmoc-*S*,*S*-4-(*S*)-MTPA.** The procedures applied to the synthesis of *N*-Fmoc-S*,*S*-4-(*S*)-MTPA** used *N*-Fmoc-***S*,*S*-4** (10 mg, 0.027 mmol), pyridine (10 µL, 0.1 mmol) and (*R*)-Mosher chloride (20 µL, 0.1 mmol) to obtain the product as a white solid (15 mg, 97% yield). ^{1}H NMR (400 MHz, $CDCl_3$) δ: 7.77 (d, *J* = 7.5 Hz 2H), 7.57 (d, *J* = 7.5 Hz 2H), 7.28 -7.50 (m, 9H), 5.12-5.20 (m, 1H), 4.41-4.53 (m, 3H), 4.20 (t, *J* = 6.2 Hz 1H), 3.84 (t, *J* = 10.2 Hz 1H), 3.54 (s, 3H), 2.25-2.48 (m, 2H), 1.99 (s, 3H), 1.73-1.84 (m, 1H), 1.35-1.45 (m, 1H), 1.34 (d, *J* = 6.3 Hz 3H). HRMS $[M+H]^+$ calculated for $C_{31}H_{33}F_3NO_5S$ 588.2026, found 588.2020.

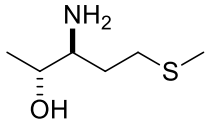

(2*R*,3*S*)-3-Amino-5-(methylthio)pentan-2-ol (*R*,*S*-metolMe, *R*,*S*-4). The procedures applied to the synthesis of (2*R*,3*S*)-3-amino-5-(methylthio)pentan-2-ol used *N*-Fmoc-***R*,*S*-4** (10 mg, 0.027 mmol) to obtain the product as a colorless oil (6 mg, 63% yield). ^{1}H NMR (400 MHz, $CDCl_3$) δ: 3.84-3.96 (m, 1H), 3.20-3.29 (m, 1H), 2.69-2.81 (m, 2H), 2.13 (s, 3H), 1.85-2.05 (m, 2H), 1.33 (d, *J* = 5.8 Hz 3H). ^{13}C NMR (100 MHz, $CDCl_3$) δ: 71.3, 59.2, 50.7, 29.9, 28.5, 15.3. HRMS $[M+H]^+$ calculated for $C_6H_{16}NOS$ 150.0947, found 150.0943.

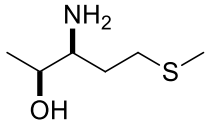

(2*S*,3*S*)-3-Amino-5-(methylthio)pentan-2-ol (*S*,*S*-metolMe, *S*,*S*-4). The procedures applied to the synthesis of (2*S*,3*S*)-3-amino-5-(methylthio)pentan-2-ol used *N*-Fmoc-***S*,*S*-4** (25 mg, 0.067 mmol) to obtain the product as a colorless oil (10 mg, 78% yield). ^{1}H NMR (400 MHz, $CDCl_3$) δ: 4.15-4.25 (m, 1H), 3.43-3.52 (m, 1H), 2.61-2.81 (m, 2H), 2.13 (s, 3H), 1.96-2.08 (m, 1H), 1.82-1.95 (m, 1H), 1.27 (d, *J* = 6.7 Hz 3H). ^{13}C NMR (100 MHz, $CDCl_3$) δ: 71.2, 59.3, 50.5, 29.8, 28.5, 15.2. HRMS $[M+H]^+$ calculated for $C_6H_{16}NOS$ 150.0947, found 150.0945.

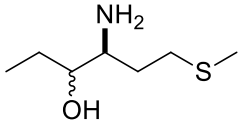

(4*S*)-4-Amino-6-(methylthio)hexan-3-ol (metolEt, 5). Ethyl magnesium bromide (1 M in THF) (1 mL, 1 mmol) was used to obtain the diastereomeric mixture of the product as a colorless oil (27 mg, 4 steps, 18% yield). ^{1}H NMR (400 MHz, $CDCl_3$) δ: 3.37-3.44 (m, 1H), 2.87-2.95 (m, 1H), 2.49-2.71 (m, 2H), 2.10 (s, 3H), 1.71-1.81 (m, 1H), 1.49-1.61 (m, 1H), 1.35-1.48 (m, 2H), 0.98 (t, *J* = 7.5 Hz 3H). ^{13}C NMR (100 MHz, $CDCl_3$) δ: 69.2, 67.2, 51.0, 30.0, 28.7, 15.4, 15.2. HRMS $[M+H]^+$ calculated for $C_7H_{18}NOS$ 164.1104, found 164.1105.

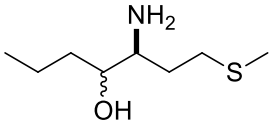

(3*S*)-3-Amino-1-(methylthio)heptan-4-ol (metolPr, 6). *n*-Propyl magnesium bromide (1 M in THF) (1 mL, 1 mmol) was used to obtain the diastereomeric mixture of the product as a colorless oil (29 mg, 4 steps, 15% yield). ^{1}H NMR (400 MHz, $CDCl_3$) δ: 3.93-4.00 (m, 1H), 3.33-3.42 (m, 1H), 2.63-2.85 (m, 2H), 2.13 (s, 3H), 1.83-2.05 (m, 2H), 1.45-1.64 (m, 2H), 1.29-1.43 (m, 2H), 0.95 (t, *J* = 7.0 Hz 3H). ^{13}C NMR (100 MHz, $CDCl_3$) δ: 73.1, 69.0, 50.5, 29.6, 28.3, 22.4, 14.9, 10.3. HRMS $[M+H]^+$ calculated for $C_8H_{20}NOS$ 178.1260, found 178.1258.

4. Protein crystallization, data collection, and structure refinement.

Large scale expression and purification of the hMAT2A-K289L mutant followed the same protocol as the wild type.[3] Purified hMAT2A-K289L mutant protein at a concentration of 10-20 mg mL^{-1} in a buffer containing 50mM HEPES, pH 7.5, 10 mM Metol, 5 mM magnesium chloride, 2 mM ADP was mixed with a reservoir solution in a 200 nL:200 nL sitting drop crystallization trail. Hits were obtained using the Index-HT screen (Hampton Research, Aliso Viejo, CA) setup with a Mosquito liquid handling robot (TTP Labtech). The best crystals were produced using a reservoir containing 0.2 M KCl, 0.05 M HEPES pH7.5, 35% (v/v) pentaeythritol propoxylate (5/4 PO/OH). They were harvested after 7 months using 100 μm Dual Thickness MicroMounts (MiTeGen, Ithaca, NY) under silicon oil (Hampton Research, Aliso Viejo, CA) and plunge-cooled in liquid nitrogen. Data were collected with a Rayonix MX-300 CCD detector (Evanston, IL) on LS-CAT beamline 21-ID-F at the Advanced Photon Source (APS, Argonne National Lab). Data were integrated, reduced and scaled using *XDS*[4,5] followed by anisotropic analysis, elliptical truncation and merging using *STARANISO*.[6] The resolution limits of the cutoff surface were 2.8 Å, 1.8 Å and 2.1 Å along the a*, b* and c* axes with a maximum resolution limit of 2.05 Å. Since the data are incomplete to 2.05 Å, we define the nominal resolution as 2.30 Å, which is the resolution of a dataset that is 100% complete and has the same number of reflections as observed in dataset after applying the cutoff.[7] Nevertheless, there are 2618 reflections observed between 2.05 and 2.30 Å (39.1% complete for this shell) included in the refinement. Model completion and refinement were performed with *Coot*,[8] *phenix.refine*[9] and *Buster*.[10] The crystals were isomorphous with the higher resolution wild-type structure (PDB: 2p02),[11] which was used for the initial phasing. Refinement included torsion-angle, reference model restraints derived from the 2p02 structure and TLS refinement with one TLS group for the protein. Comparison of the final model to the 2p02 reference model has an RMSD 0.34 for all 2983 matching atoms and 0.25 for the 393 matching Cα atoms. Data-reduction and refinement statistics are summarized in supplemental Table S1 and binding pocket density is shown in Figure S3.

5. Supplementary references.

(1) Huber, T. D., Wang, F., Singh, S., Johnson, B. R., Zhang, J., Sunkara, M., Van Lanen, S. G., Morris, A. J., Phillips, G. N., and Thorson, J. S. (2016) Functional AdoMet isosteres resistant to classical AdoMet degradation pathways. *ACS Chem. Biol. 11*, 2484–2491.

(2) Hoye, T. R., Jeffrey, C. S., and Shao, F. (2007) Mosher ester analysis for the determination of absolute configuration of stereogenic (Chiral) carbinol carbons. *Nat. Protoc. 2*, 2451–2458.

(3) Singh, S., Zhang, J., Huber, T. D., Sunkara, M., Hurley, K., Goff, R. D., Wang, G., Zhang, W., Liu, C., Rohr, J., Van Lanen, S. G., Morris, A. J., and Thorson, J. S. (2014) Facile chemoenzymatic strategies for the synthesis and utilization of *S*-adenosyl-L-methionine analogues. *Angew. Chemie Int. Ed. 53*, 3965–3969.

(4) Kabsch, W. (2010) XDS. *Acta Crystallogr. D66*, 125–132.

(5) Kabsch, W. (2010) Integration, scaling, space-group assignment and post-refinement. *Acta Crystallogr. D66*, 133–144.

(6) Tickle, I. J., Flensburg, C., Keller, P., Paciorek, W., Sharff, A., Vonrhein, C., and Bricogne, G. (2018) STARANISO. *http://staraniso.globalphasing.org/cgi-bin/staraniso.cgi*. Global Phasing Ltd., Cambridge, United Kingdom.

(7) Kleywegt, G. J. (2000) Validation of protein crystal structures. *Acta Crystallogr. D56*, 249–265.

(8) Emsley, P., Lohkamp, B., Scott, W. G., and Cowtan, K. (2010) Features and development of Coot. *Acta Crystallogr. D. Biol. Crystallogr. 66*, 486–501.

(9) Adams, P. D., Afonine, P. V, Bunkóczi, G., Chen, V. B., Davis, I. W., Echols, N., Headd, J. J., Hung, L.-W., Kapral, G. J., Grosse-Kunstleve, R. W., McCoy, A. J., Moriarty, N. W., Oeffner, R., Read, R. J., Richardson, D. C., Richardson, J. S., Terwilliger, T. C., and Zwart, P. H. (2010) PHENIX: A comprehensive Python-based system for macromolecular structure solution. *Acta Crystallogr. D66*, 213–221.

(10) Bricogne, G., Blanc, E., Brandl, M., Flensburg, C., Keller, P., Paciorek, W., Roversi, P., Sharff, A., Smart, O. S., Vonrhein, C., and Womack, T. O. (2017) BUSTER. Global Phasing Ltd., Cambridge, United Kingdom.

(11) Shafqat, N., Muniz, J. R. C., Pilka, E. S., Papagrigoriou, E., von Delft, F., Oppermann, U., and Yue, W. W. (2013) Insight into *S*-adenosylmethionine biosynthesis from the crystal structures of the human methionine adenosyltransferase catalytic and regulatory subunits. *Biochem. J. 452*, 27–36.

(12) Liebschner, D., Afonine, P. V., Moriarty, N. W., Poon, B. K., Sobolev, O. V., Terwilliger, T. C., and Adams, P. D. (2017) Polder maps: improving OMIT maps by excluding bulk solvent. *Acta Crystallogr. D73*, 148–157.

(13) Diederichs, K., and Karplus, P. A. (1997) Improved R-factors for diffraction data analysis in macromolecular crystallography. *Nat. Struct. Biol. 4*, 269–275.

(14) Chen, V. B., Arendall, W. B., Headd, J. J., Keedy, D. A., Immormino, R. M., Kapral, G. J., Murray, L. W., Richardson, J. S., and Richardson, D. C. (2010) MolProbity: All-atom structure validation for macromolecular crystallography. *Acta Crystallogr. D66*, 12–21.

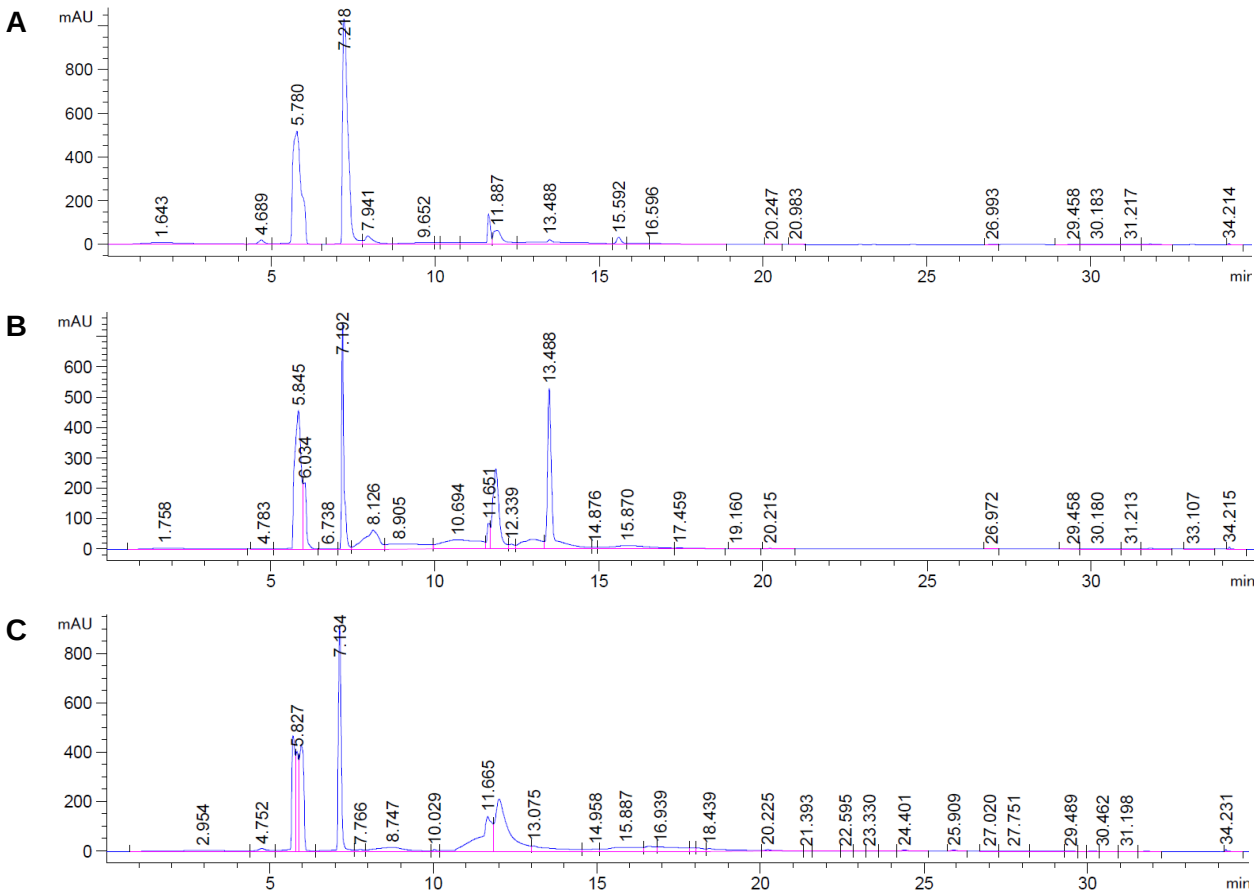

Figure S1. Representative analytical HPLC at A_{260}. (A) hMAT2A mutant K289L (10 µM) with 10 mM metol and 2 mM ATP after 24 hr, highlighting the lack of MTA (13.5 min) production. (B) hMAT2A mutant K289L (10 µM) with 10 mM L-Met and 2 mM ATP after 24 hr, highlighting notable production of MTA (13.5 min). (C) hMAT2A mutant K289F (10 µM) with 10 mM *R*,*S*-metolMe and 2 mM ATP after 24 hr, highlighting the lack of MTA (13.5 min) production. AdoMet analogues (5.8 min), adenine (7.2 min), ATP (11.6 min), MTA (13.5 min).

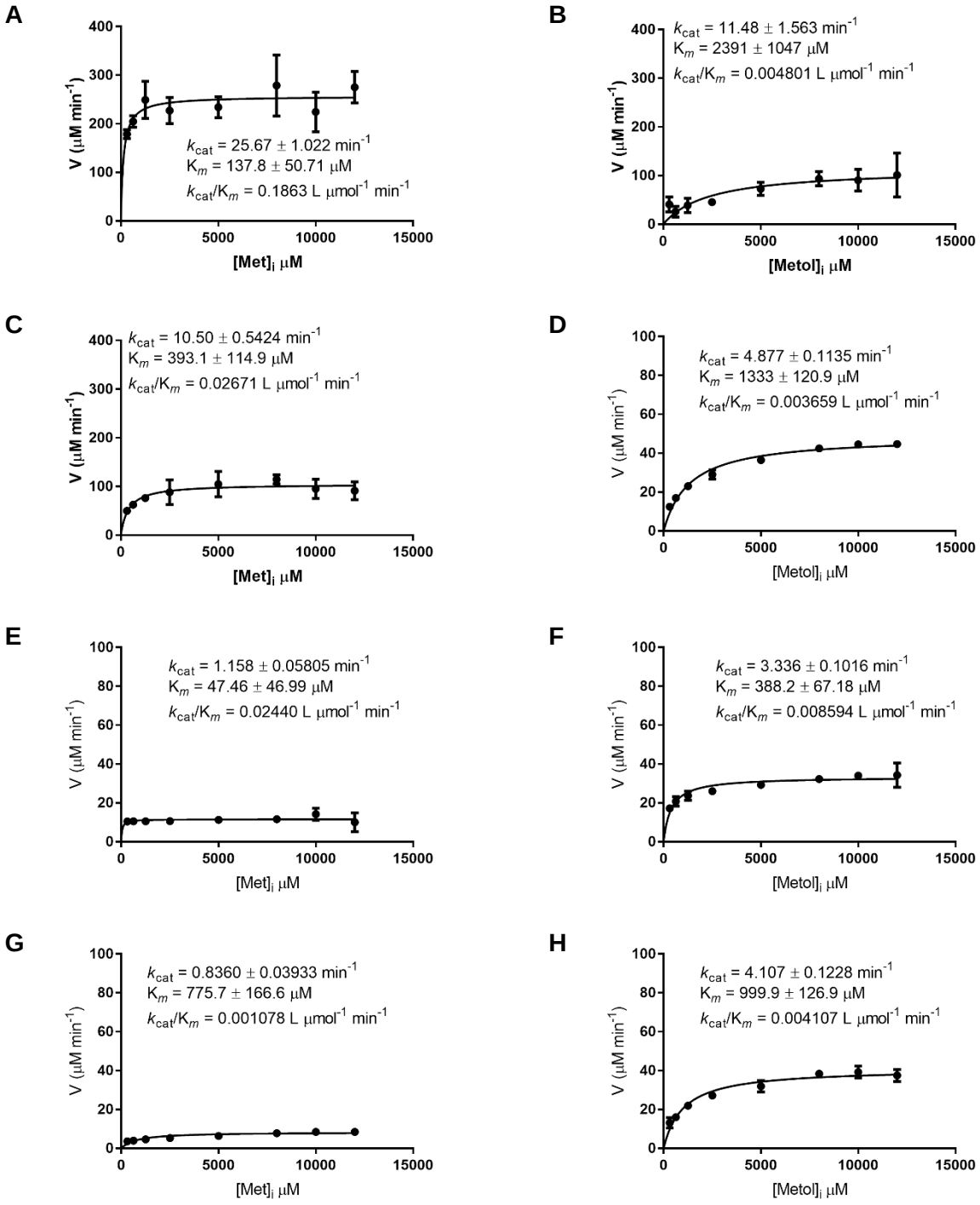

Figure S2. Determination of kinetic parameters for mutant and wt-hMAT2A-catalyzed reactions. [hMAT2A or hMAT2A mutant] = 10 μM and [ATP]$_i$ = 2000 μM in all experiments. **(A)** wt-hMAT2A, [Met]$_i$ = varied. **(B)** wt-hMAT2A, [Metol]$_i$ = varied. **(C)** hMAT2A mutant E70S, [Met]$_i$ = varied. **(D)** hMAT2A mutant K289S, [Metol]$_i$ = varied. **(E)** hMAT2A mutant Q113D, [Met]$_i$ = varied. **(F)** hMAT2A mutant Q113D, [Metol]$_i$ = varied. **(G)** hMAT2A mutant K289L, [Met]$_i$ = varied. **(H)** hMAT2A mutant K289L, [Metol]$_i$ = varied.

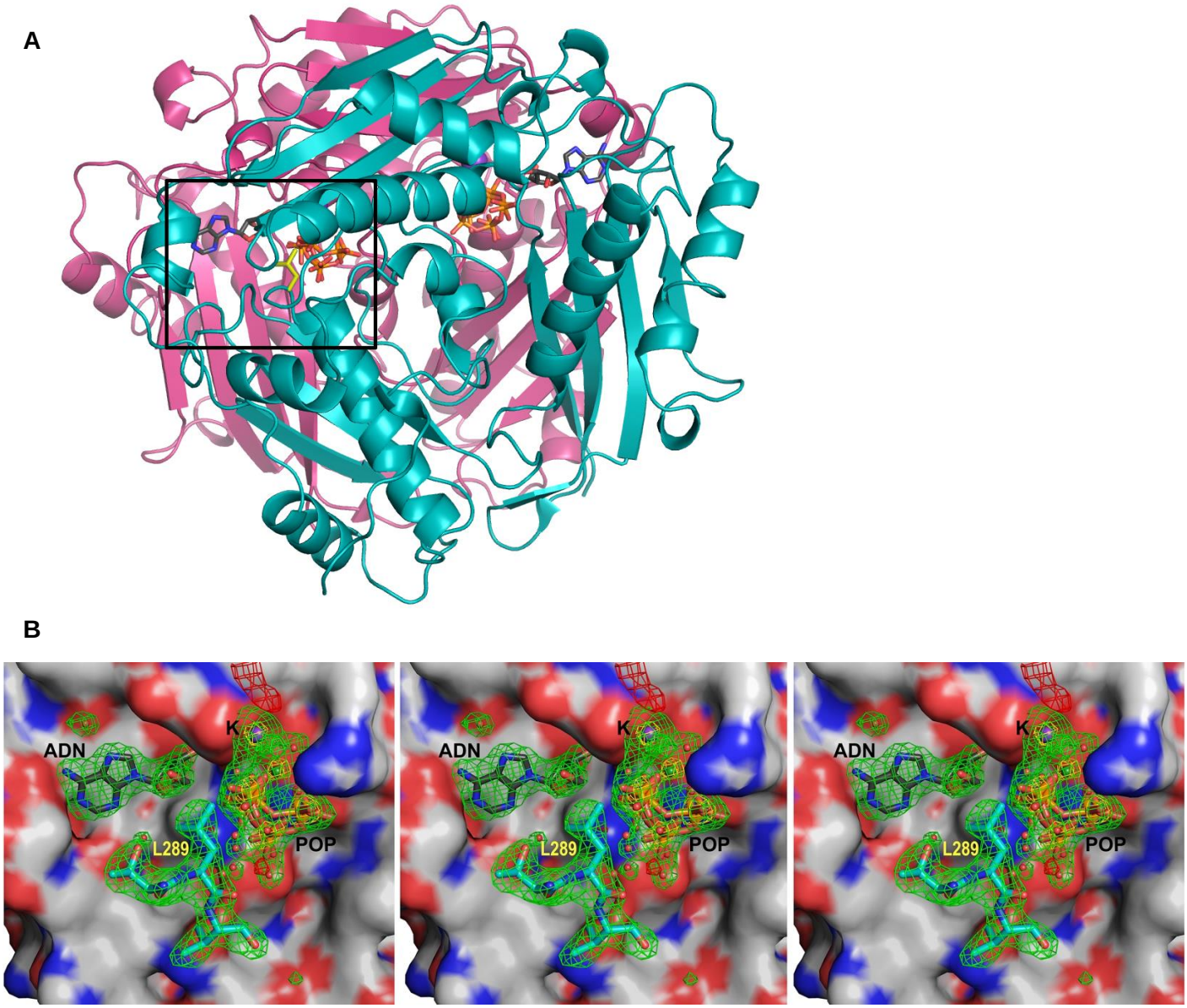

Figure S3. hMAT2A-K289L electron density map. **(A)** Ribbon diagram of the hMAT2A-K289L dimer with the L289 residue highlighted in yellow. **(B)** Stereo triptych (left-right-left) showing the hMAT2A-K289L *mFo-DFc* polder omit electron density map[12] contoured at +3.2 (green), +8.0 (yellow) and -3.2 (red) r.m.s.d. The residues adjacent to and including the mutation 288-TLV-290 (cyan carbons) as well as the adenosine (gray carbons), disordered pyrophosphate (red and orange), magnesium ion (green), potassium ion (purple) and nearby waters were omitted from the polder map calculation. The orientation is the same as (A) with the magenta protomer shown in surface representation and only the omitted 288-TLV-290 tripeptide shown from the cyan protomer for clarity.

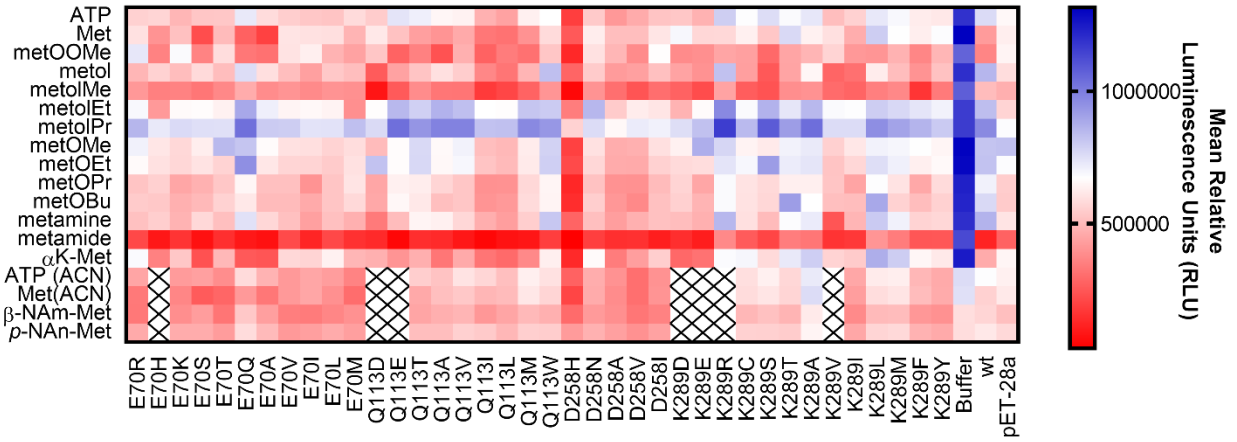

Figure S4. Combinatorial plate-based screen of targeted hMAT2A mutants with L-Met analogues highlighted in Figure 2. The heat map compares the relative activity of hMAT2A mutant (y-axis) and L-Met analogue (x-axis) pairings. The color of each square is dependent on the measured mean relative luminescence units (RLU) under experimental conditions for that mutant. Red corresponds to lower observed luminescence (*i.e.*, lower [ATP]) as an indirect measure of turnover; blue indicates higher observed luminescence (*i.e.*, higher [ATP]) as an indirect measure of lack of turnover; X, not tested. Standard assay conditions: 10 mM L-Met analogue, 1.5 mM ATP, 37 °C, 60 min.

Table S1. Summary of crystal parameters, data collection, and refinement statistics. Elliptically truncated data from *STARANISO* was used for the final refinement.

Crystal parameters	hMAT2A - K289L	
Space group	*I 2 2 2*	
Unit-cell lengths (Å)	60.6, 104.1, 63.0	
Data collection statistics	*after elliptical trimming*	*before elliptical trimming*
Wavelength (Å)	0.98	
Resolution range (Å)	40-2.05	40-2.05
High Resolution bin range (Å)	(2.22-2.05)	(2.22-2.05)
No. of observations measured	146,211 (14,326)	199,742 (37,145)
No. of unique reflections	16,840 (1,684)	23,368 (4,770)
Completeness spherical (%)	72.0 (35.9)	99.9 (99.4)
Completeness elliptical (%)	93.9 (85.7)	
R_{merge}[a]	0.194 (1.66)	0.254 (2.93)
R_{meas}[b]	0.207 (1.76)	0.270 (3.14)
Redundancy	8.7 (8.5)	8.6 (7.8)
Mean I / sigma (I)	9.3 (1.4)	6.9 (0.7)
$CC_{1/2}$[c]	1.00 (0.42)	1.00 (0.34)
Refinement and model statistics		
R_{cryst} / R_{free}[d]	0.174 / 0.203	
No. of reflections (total / test)	16,835 / 825	
RMSD bonds (Å)	0.002	
RMSD angles (°)	0.64	
No. of protein atoms	5,137	
No. of waters	158	
No. of auxiliary molecules	1 adenosine, 1 pyrophosphate, 1 magnesium ion, 1 potassium ion	
Ligands RSCC[e]	0.93 / 0.98 / 0.99 / 1.0	
B factor - protein/ligand/solvent (Å^2)	37.5 / 39.5 / 36.5	
All atom clashscore[f]	2.3	
Protein RMSD to reference 2P02 (Å all / Cα)	0.34 / 0.25	
Ramachandran plot (%)		
Favored / allowed / disallowed regions[f]	97.1 / 2.9 / 0.0	
PDB	6P9V	

[a] $R_{merge} = \sum_h \sum_i | I_i(h) - \langle I(h) \rangle | / \sum_h \sum_i I_i(h)$, where $I_i(h)$ is the intensity of an individual measurement of the reflection and $\langle I(h) \rangle$ is the mean intensity of the reflection.

[b] $R_{meas} = \sum_h [N/(N-1)]^{1/2} \sum_i | I_i(h) - \langle I(h) \rangle | / \sum_h \sum_i I_i(h)$, is the Redundancy-independent merging R factor[13]

[c] $CC_{1/2} = \sum (x - \langle x \rangle)(y - \langle x \rangle) / [\sum (x - \langle x \rangle)^2 \Sigma (y - \langle y \rangle)^2]^{1/2}$

[d] $R_{cryst} = \sum_h ||F_{obs}| - k|F_{calc}|| / \sum_h |F_{obs}|$, where F_{obs} and F_{calc} are the observed and calculated structure factor amplitudes, respectively. R_{free}, the same as R_{cryst}, but for the 4.9% of reflections chosen at random and omitted from refinement.

[e] ligand RSCC is ligand real-space correlation coefficient, which provides an objective measure of the fit of atom coordinates to electron density.

[f] as defined by *molprobity*.[14]

Spectroscopic Data

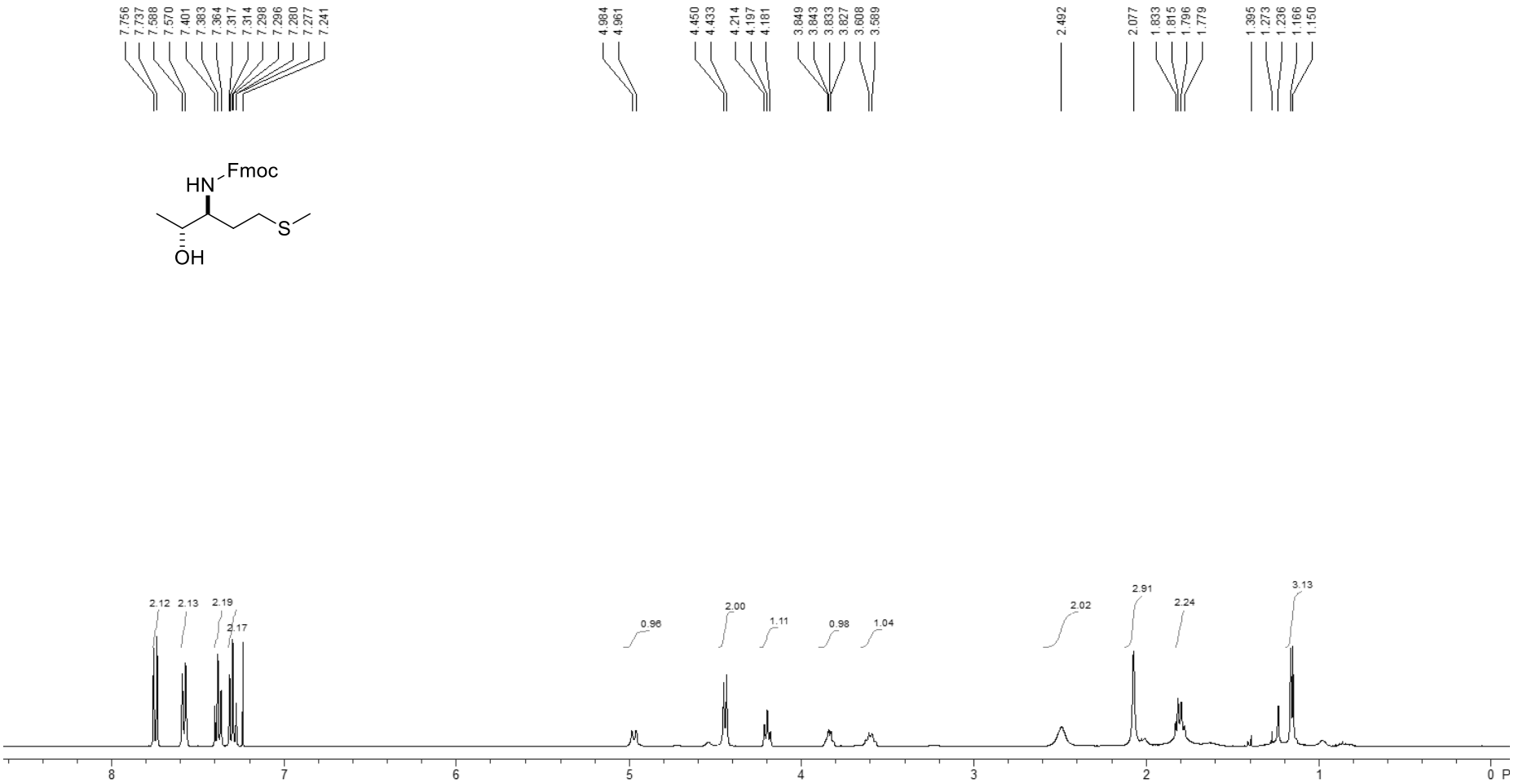

Figure S6. ^{1}H NMR (400 MHz, $CDCl_3$) of ***N*-Fmoc-*R*,*S*-4**.

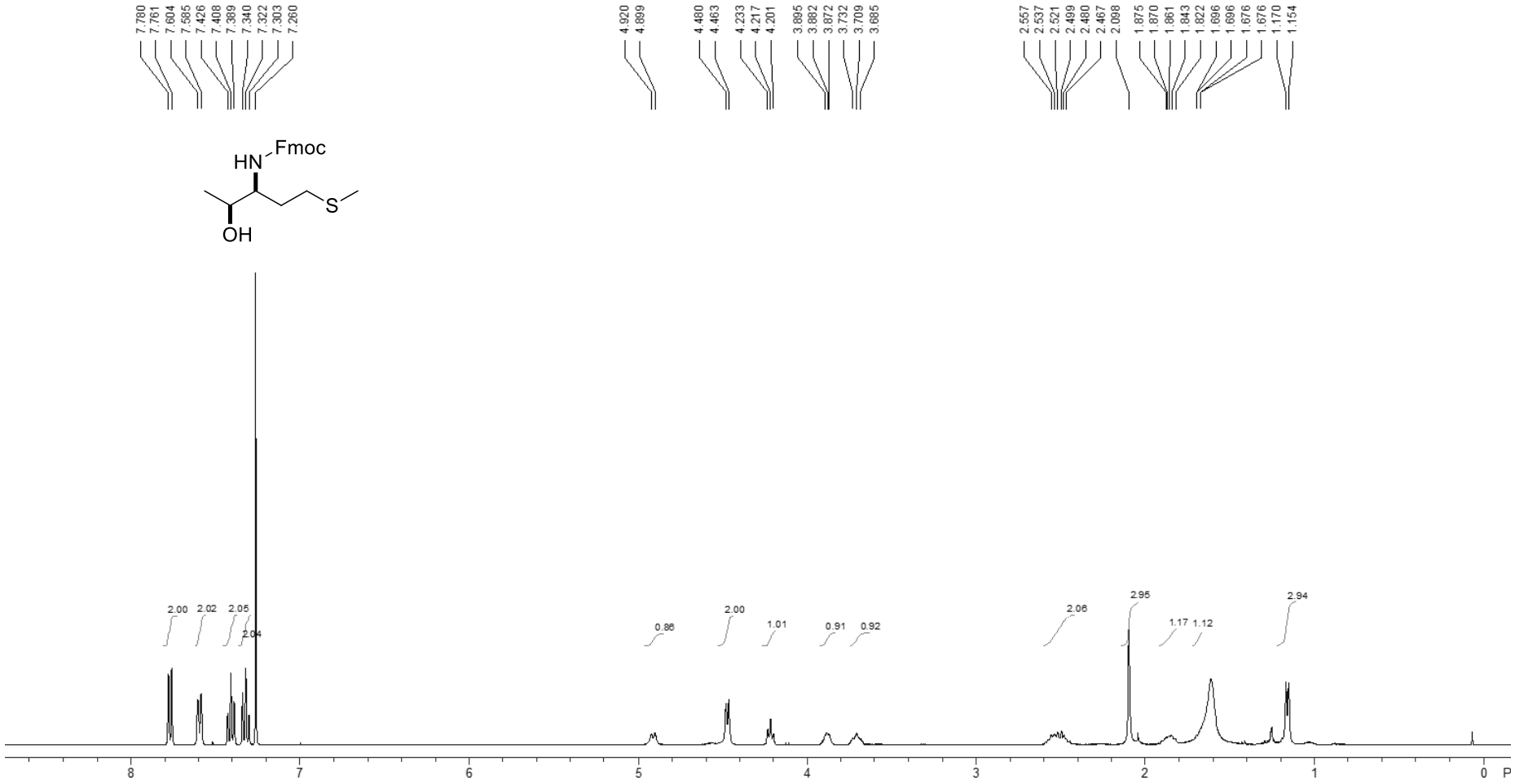

Figure S7. ^{1}H NMR (400 MHz, $CDCl_3$) of ***N*-Fmoc-*S*,*S*-4**.

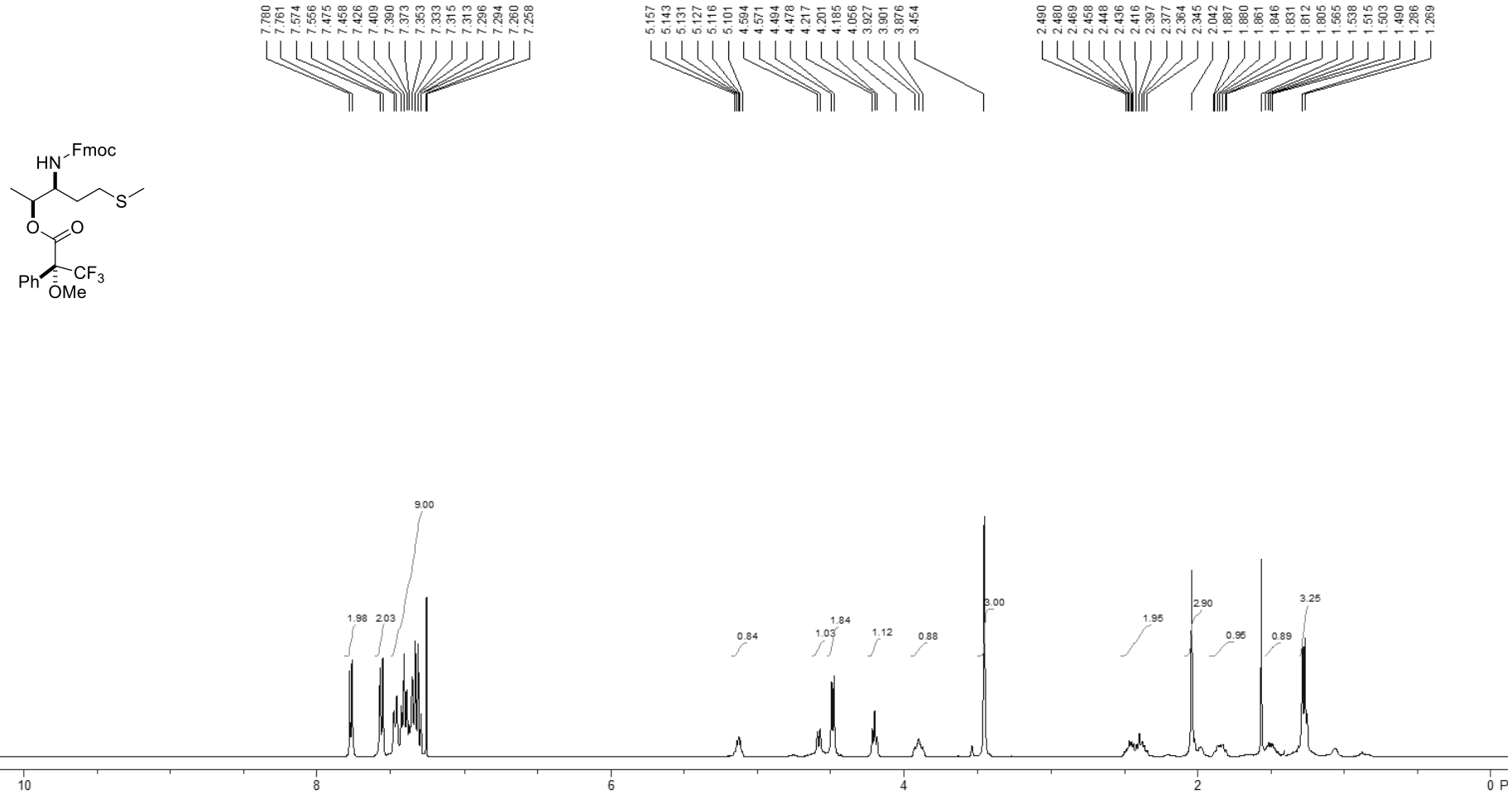

Figure S8. ^{1}H NMR (400 MHz, $CDCl_3$) of ***N*-Fmoc-*S*,*S*-4-(*R*)-MTPA**.

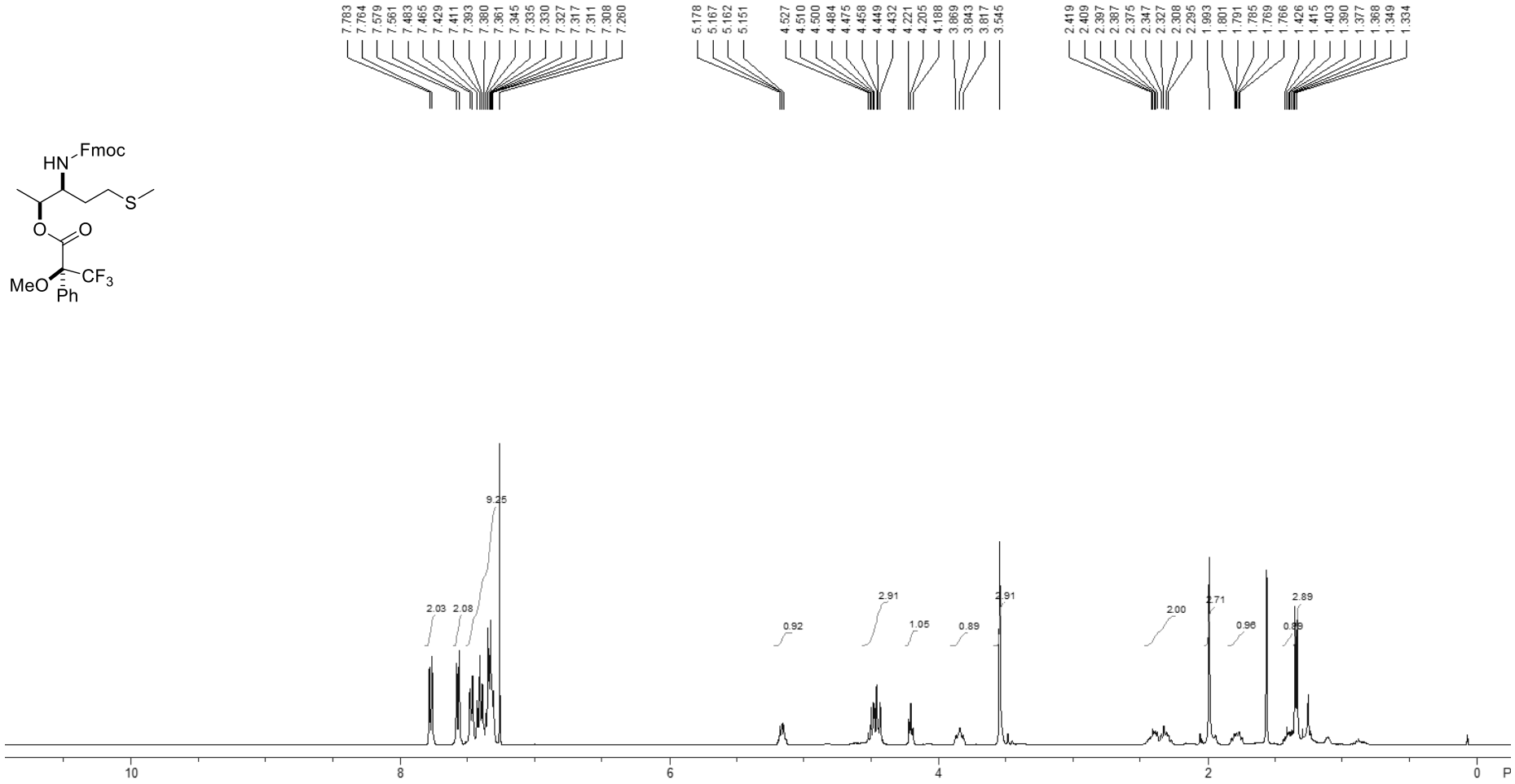

Figure S9. ^{1}H NMR (400 MHz, $CDCl_3$) of ***N*-Fmoc-*S*,*S*-4-(*S*)-MTPA**.

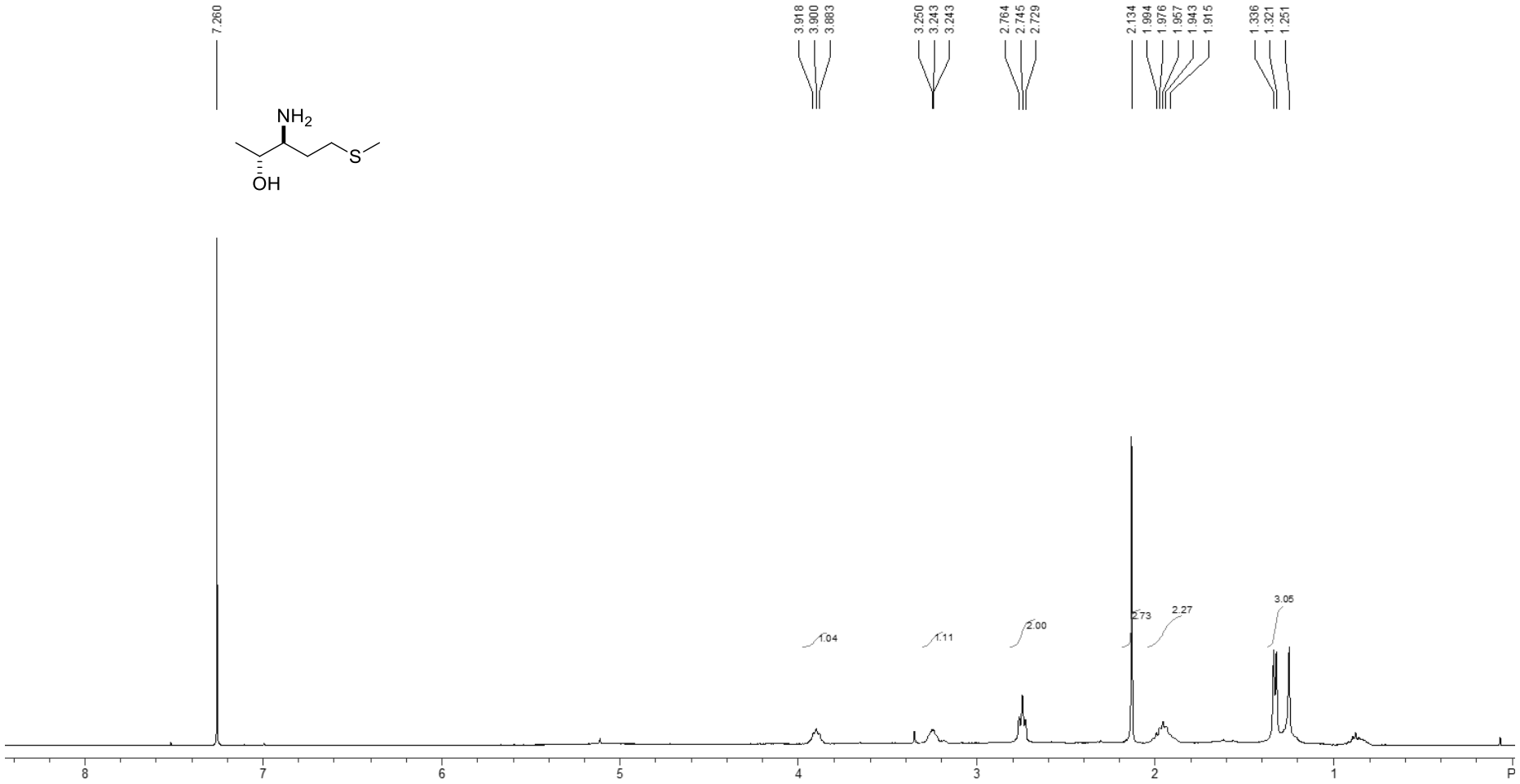

Figure S10. ^{1}H NMR (400 MHz, $CDCl_3$) of ***R*,*S*-4**.

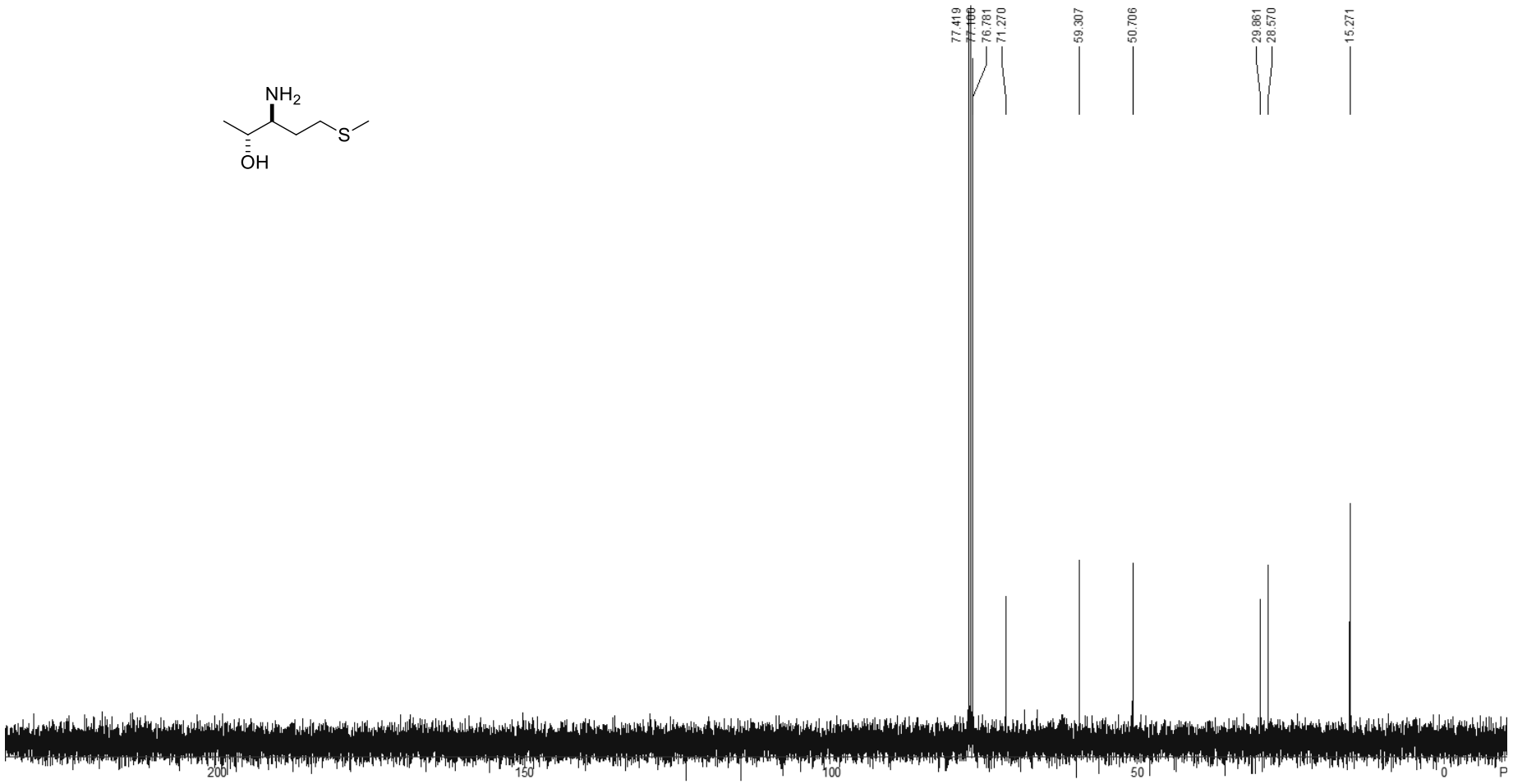

Figure S11. ^{13}C NMR (100 MHz, $CDCl_3$) of ***R*,*S*-4**.

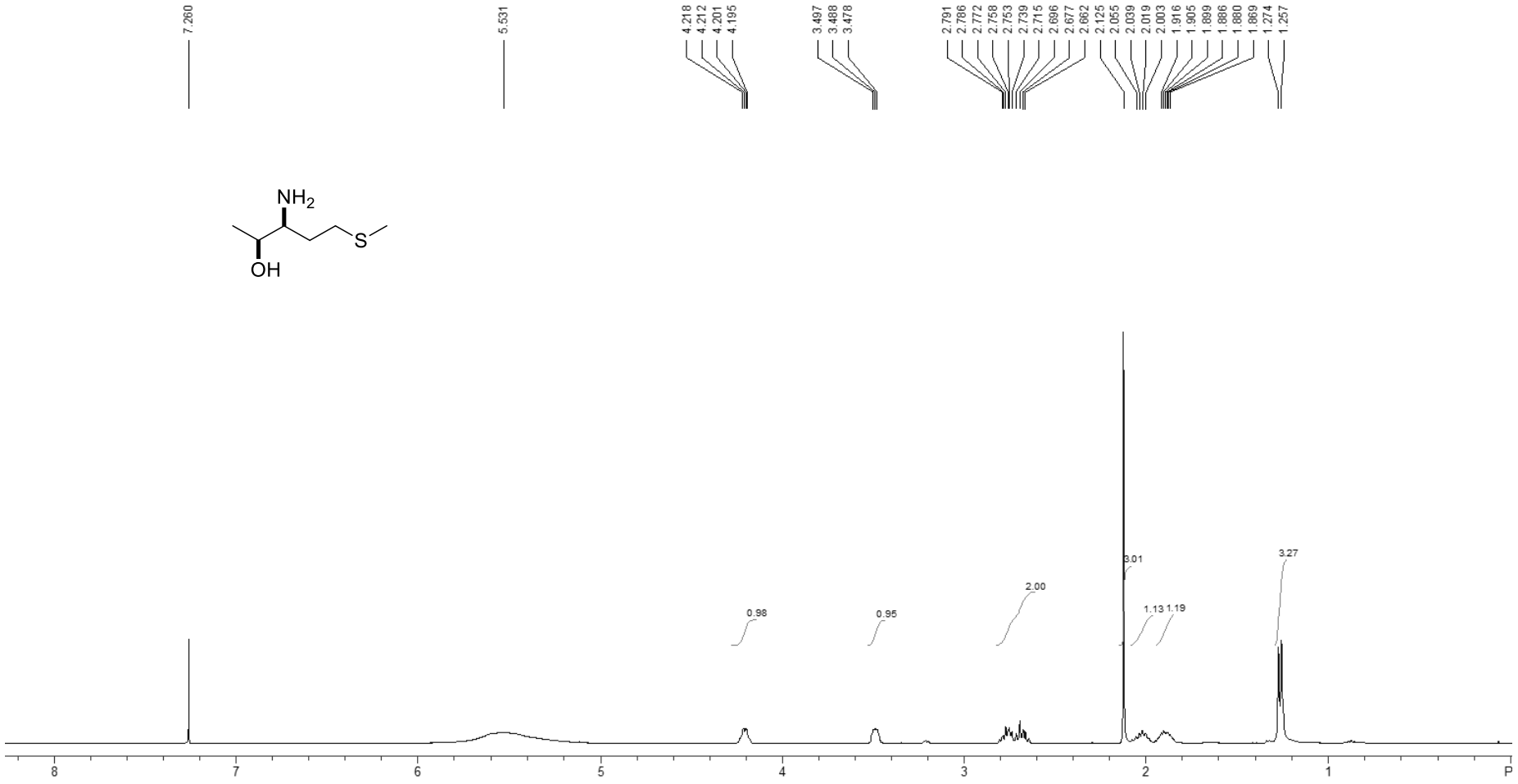

Figure S12. ^{1}H NMR (400 MHz, $CDCl_3$) of ***S,S*-4**.

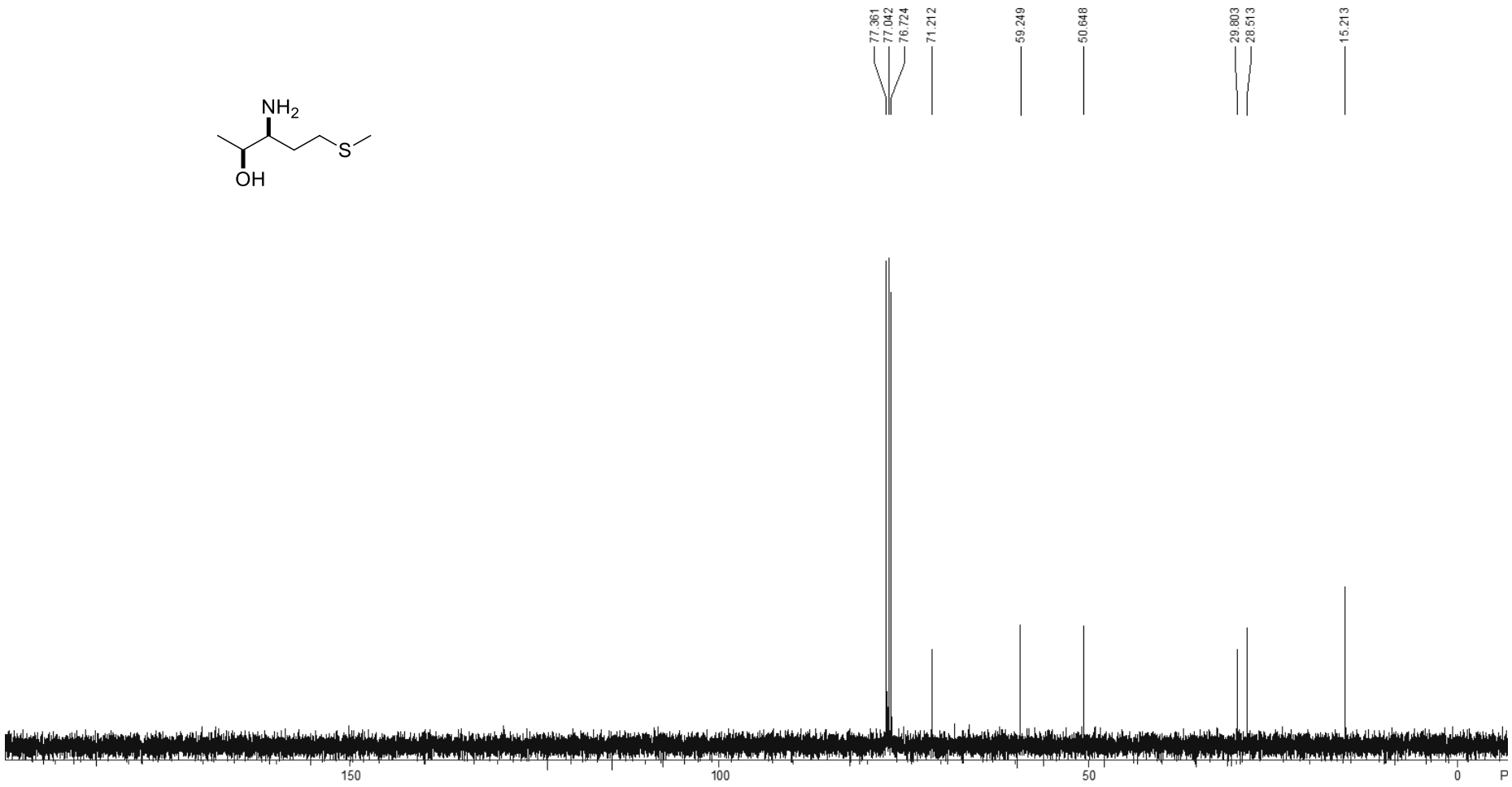

Figure S13. ^{13}C NMR (100 MHz, $CDCl_3$) of ***S,S*-4**.

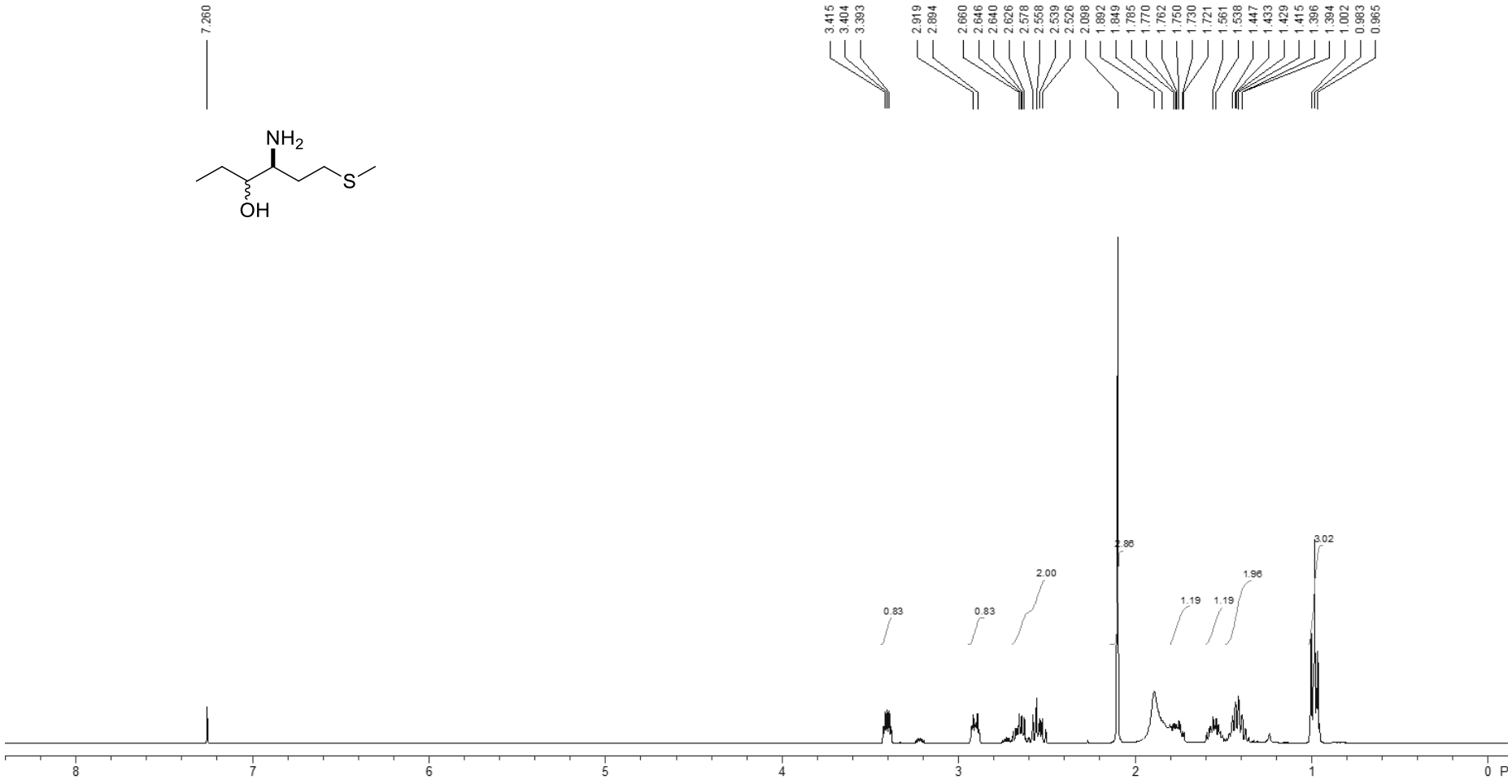

Figure S14. ^{1}H NMR (400 MHz, $CDCl_3$) of **5**.

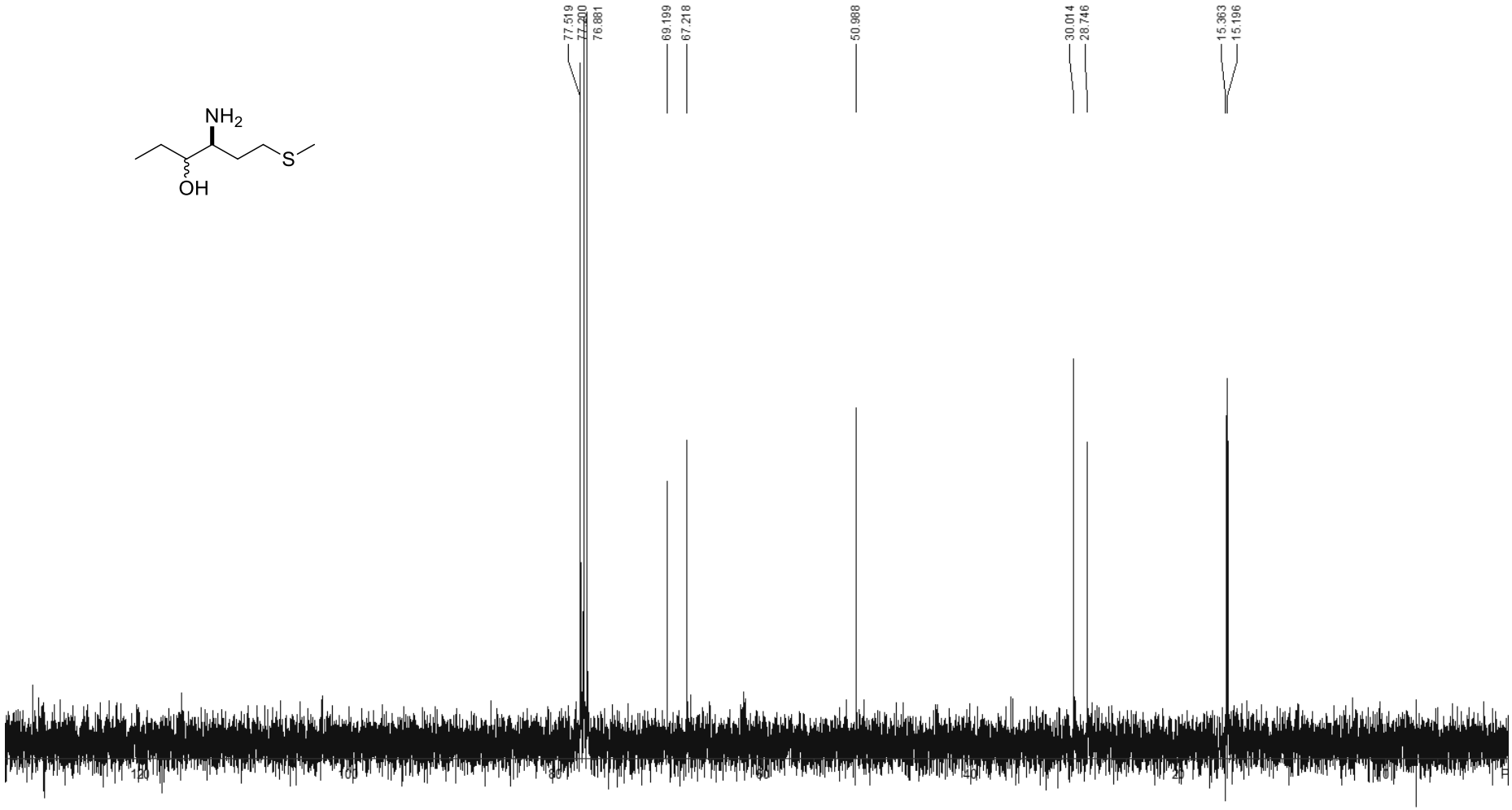

Figure S15. ^{13}C NMR (100 MHz, $CDCl_3$) of **5**.

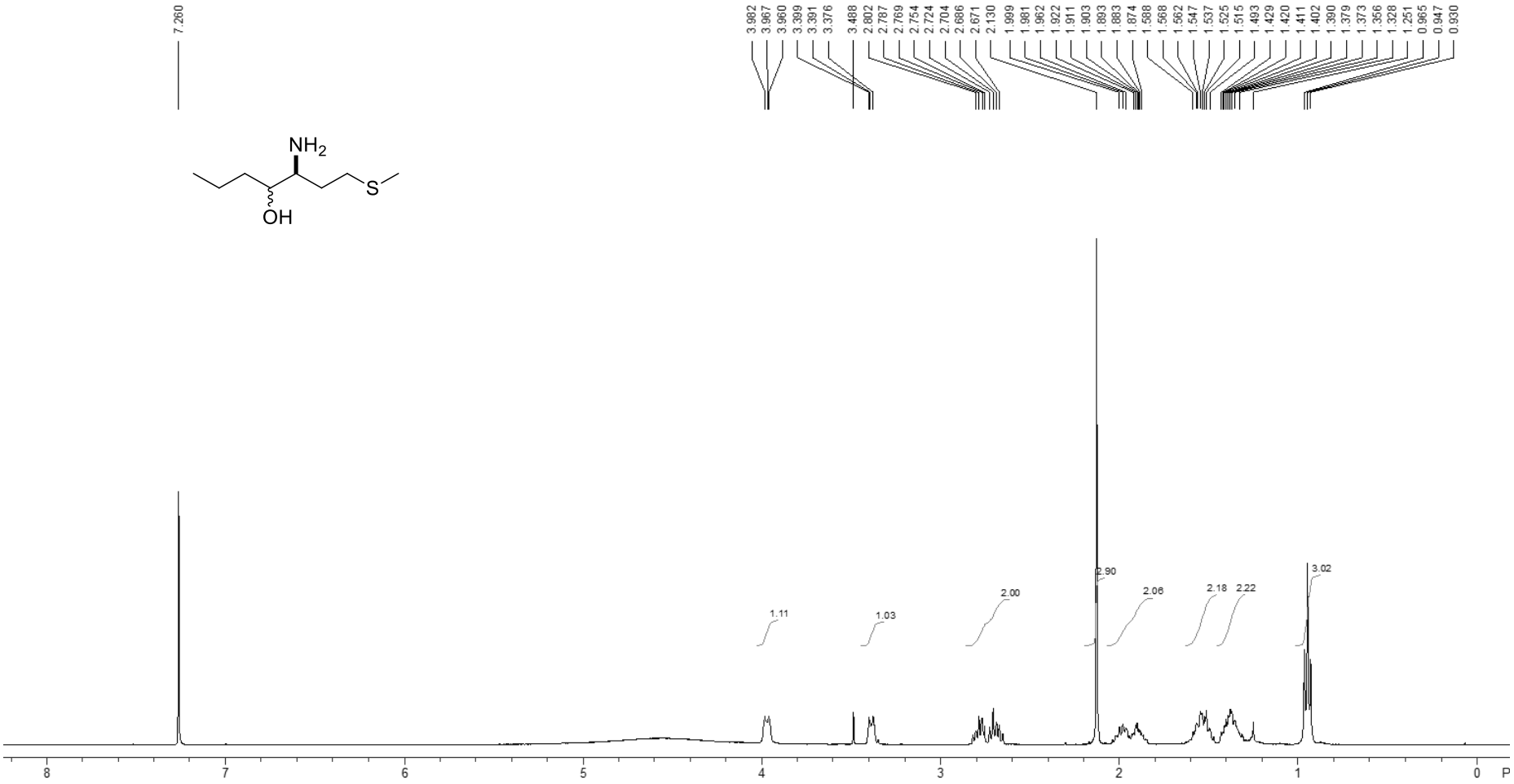

Figure S16. ^{1}H NMR (400 MHz, $CDCl_3$) of **6**.

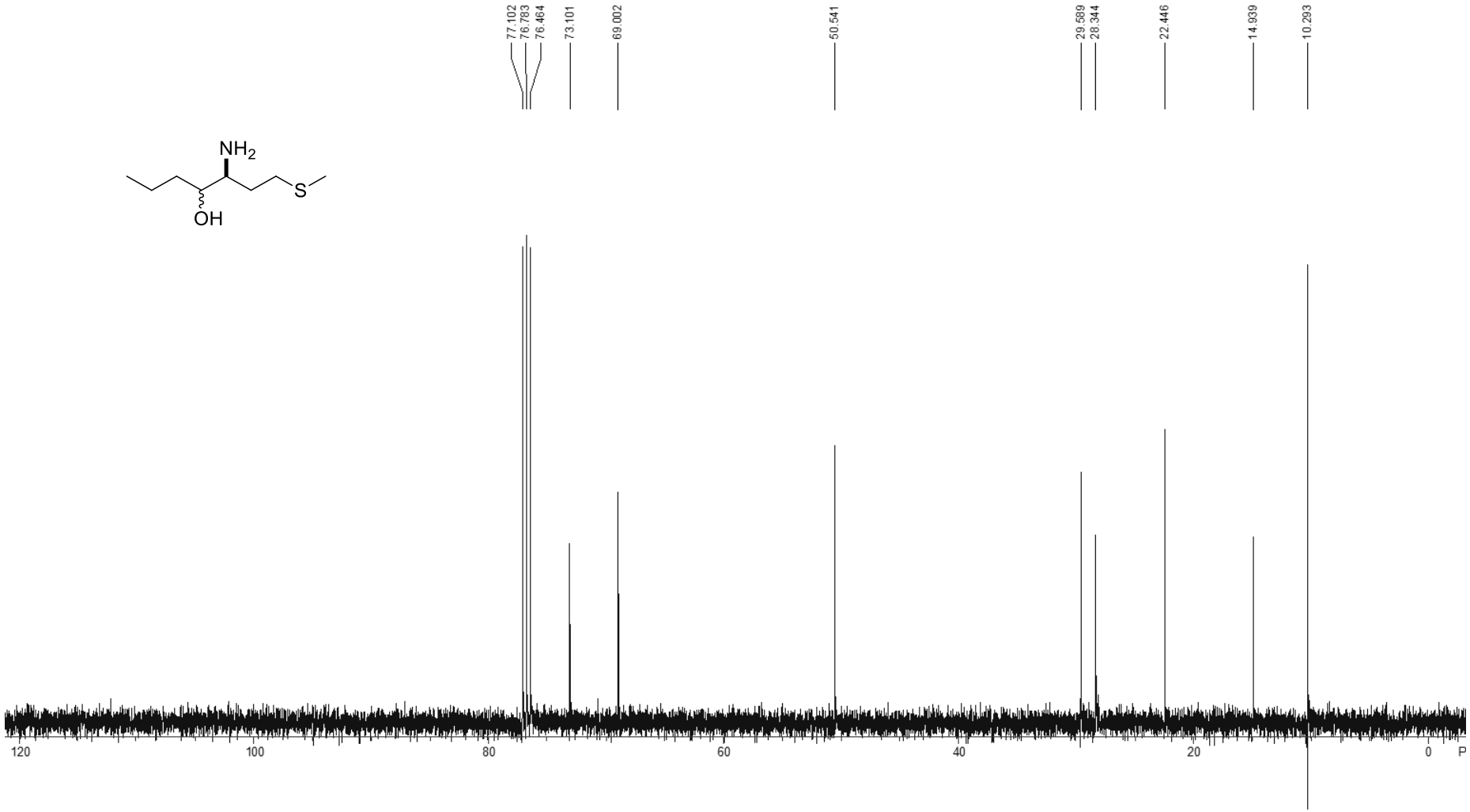

Figure S17. ^{13}C NMR (100 MHz, $CDCl_3$) of **6**.

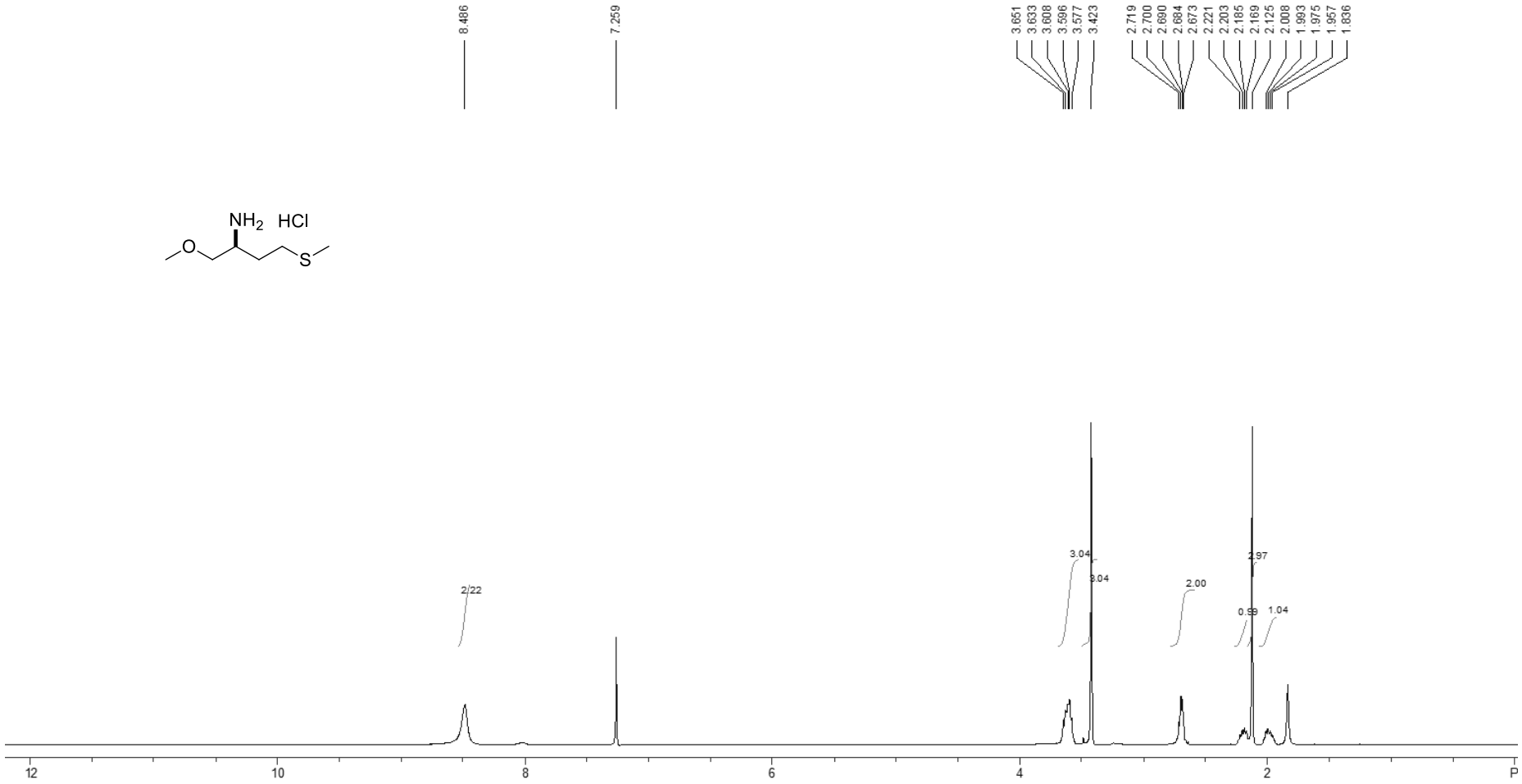

Figure S18. ^{1}H NMR (400 MHz, $CDCl_3$) of **7**.

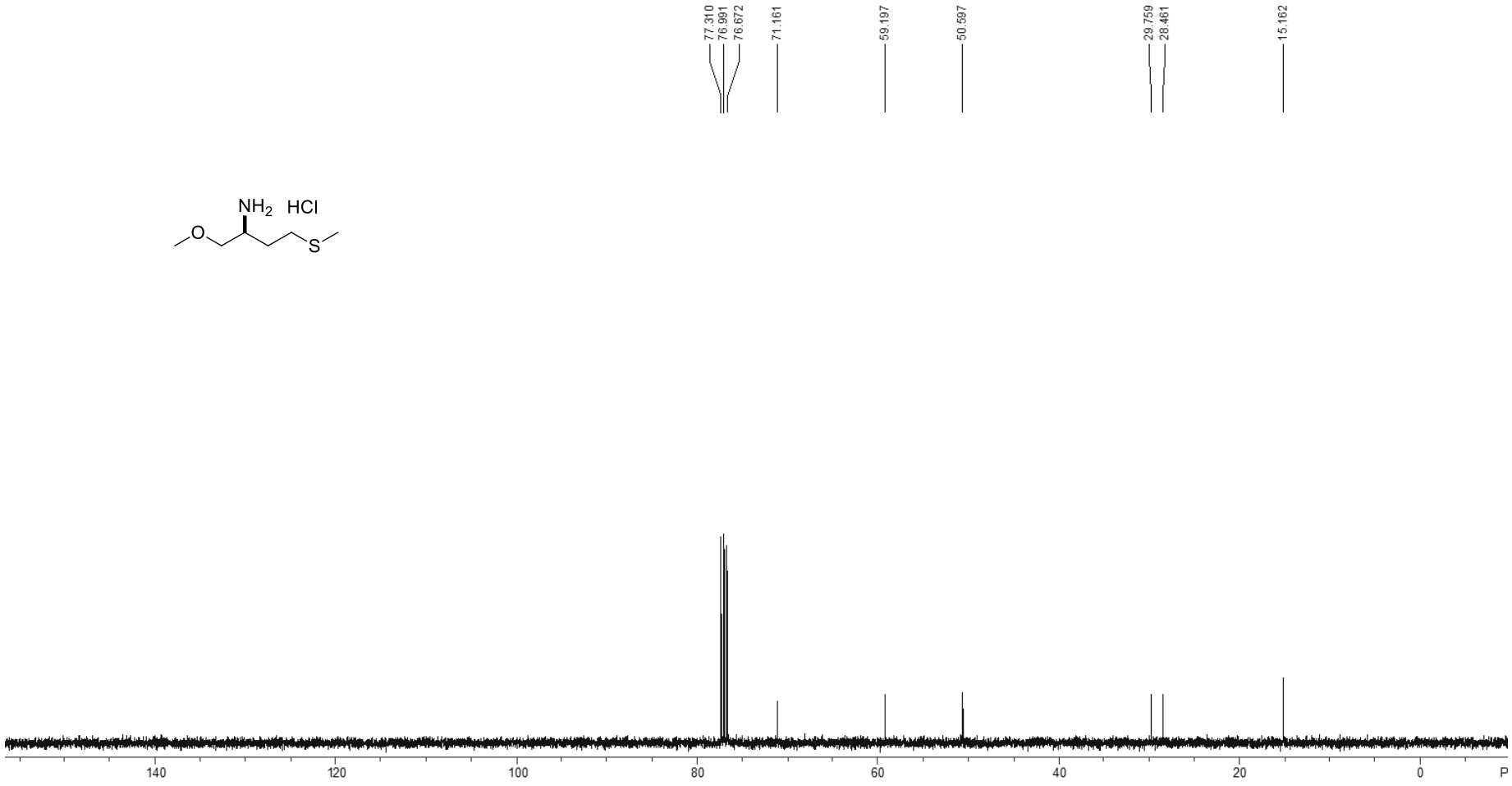

Figure S19. ^{13}C NMR (100 MHz, $CDCl_3$) of **7**.

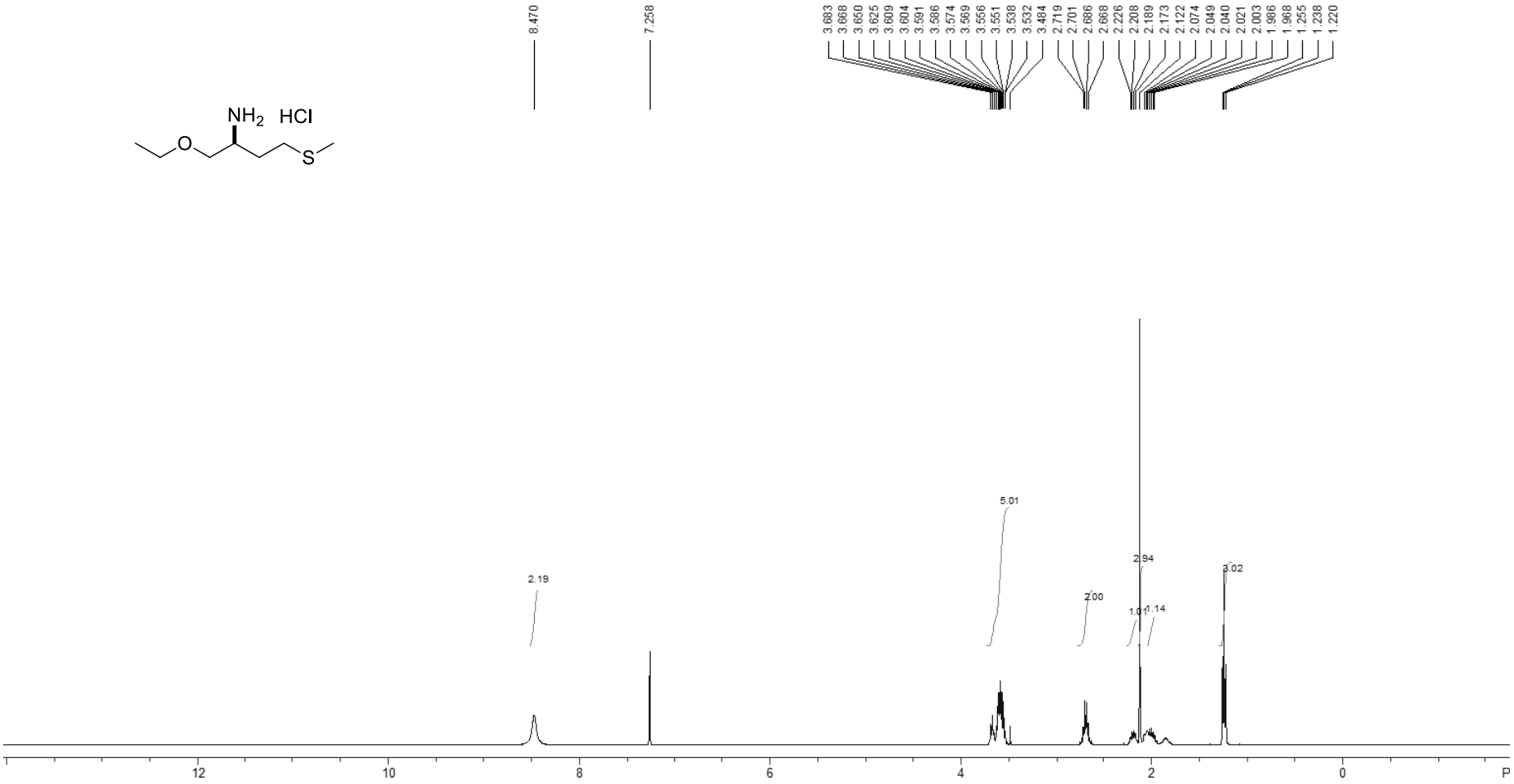

Figure S20. ^{1}H NMR (400 MHz, $CDCl_3$) of **8**.

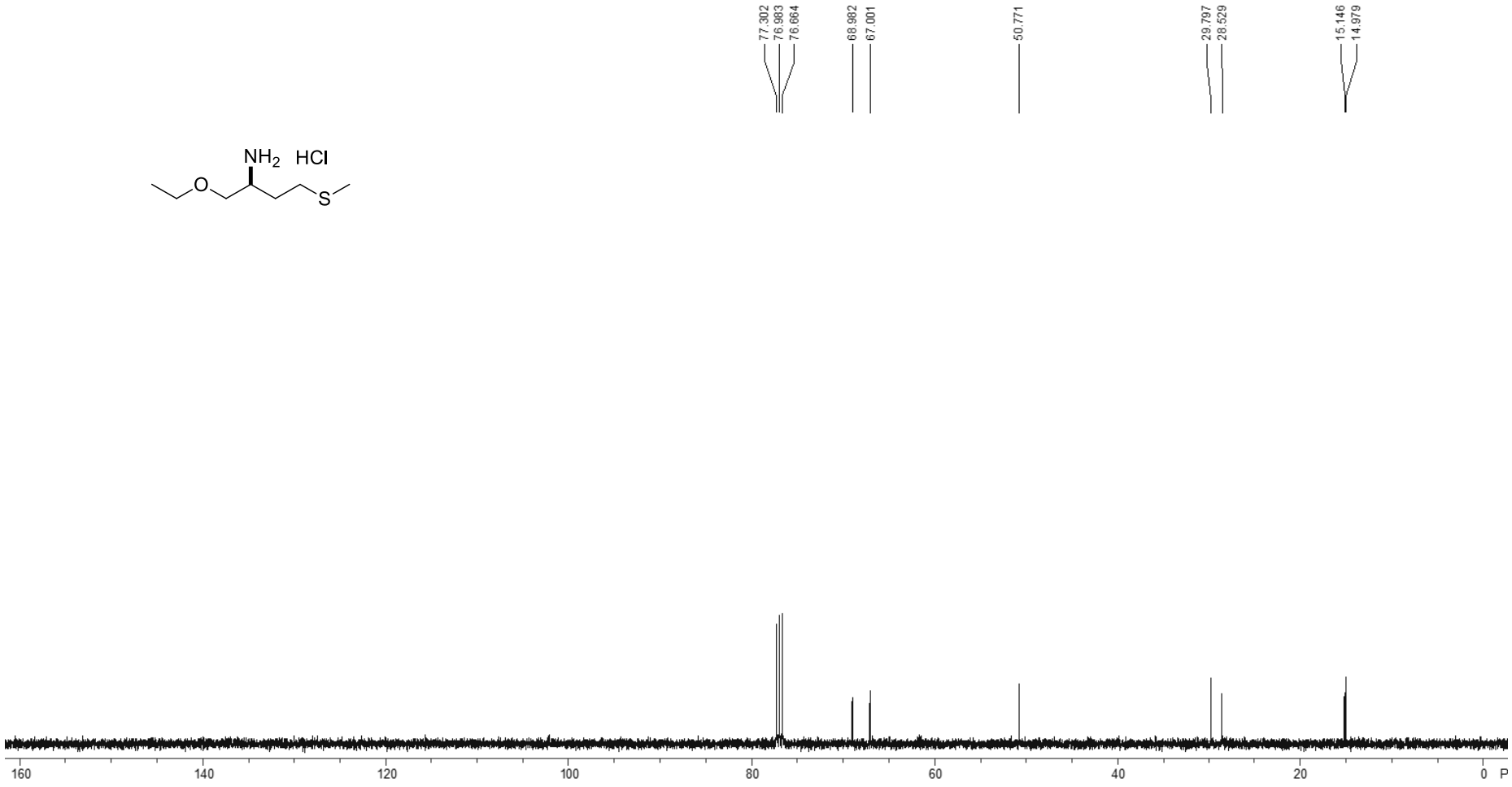

Figure S21. ^{13}C NMR (100 MHz, $CDCl_3$) of **8**.

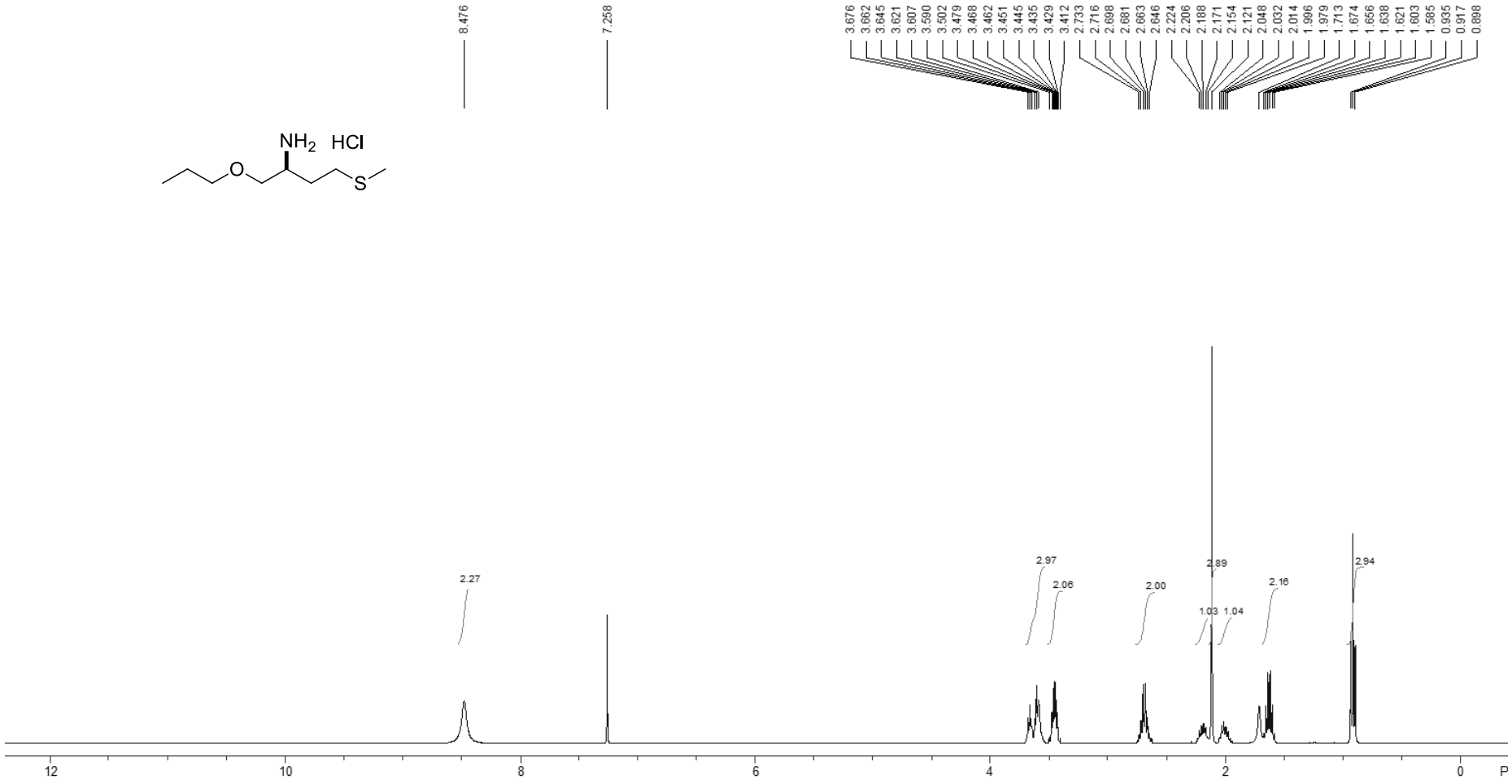

Figure S22. ^{1}H NMR (400 MHz, $CDCl_3$) of **9**.

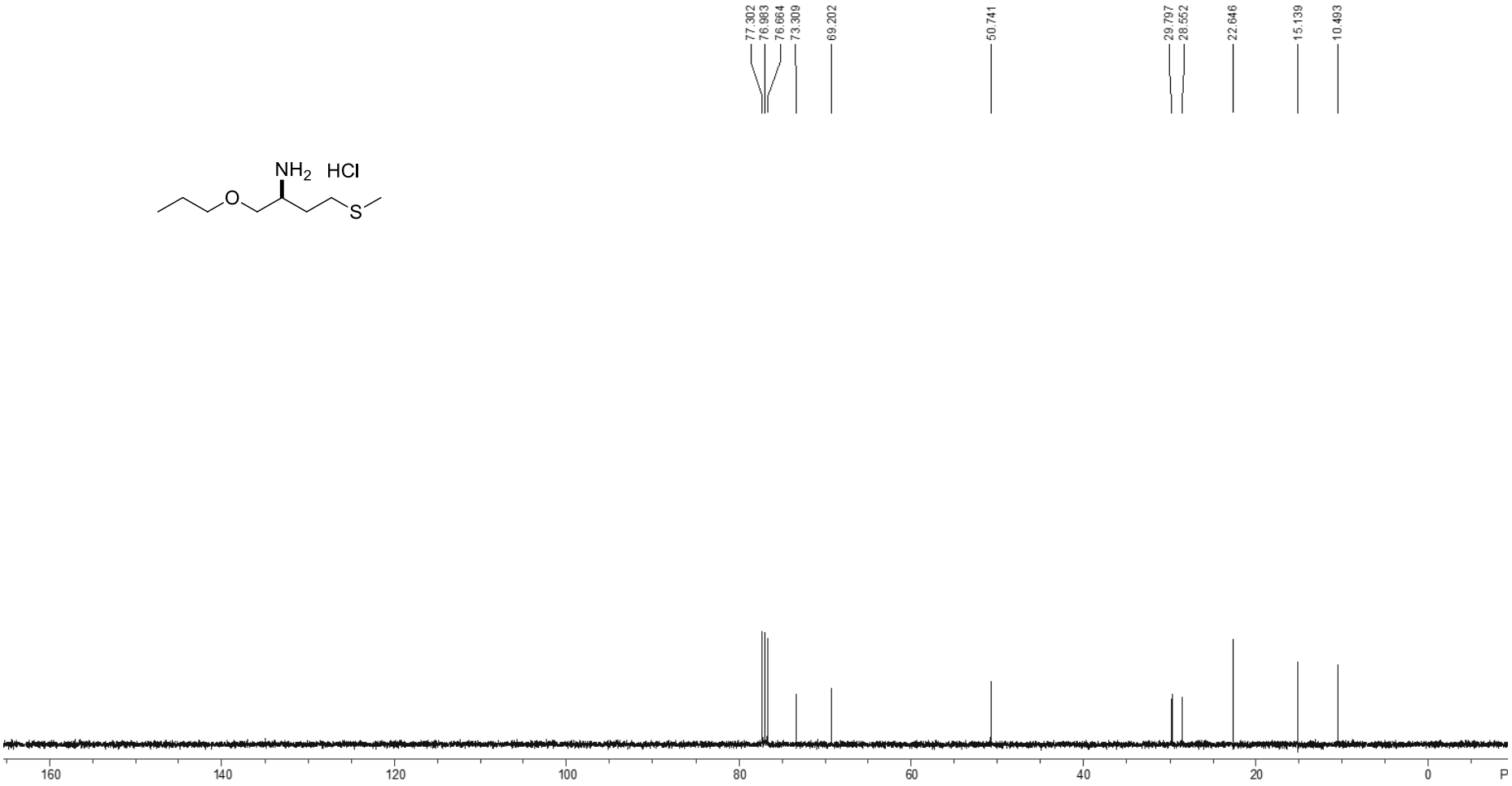

Figure S23. ^{13}C NMR (100 MHz, $CDCl_3$) of **9**.

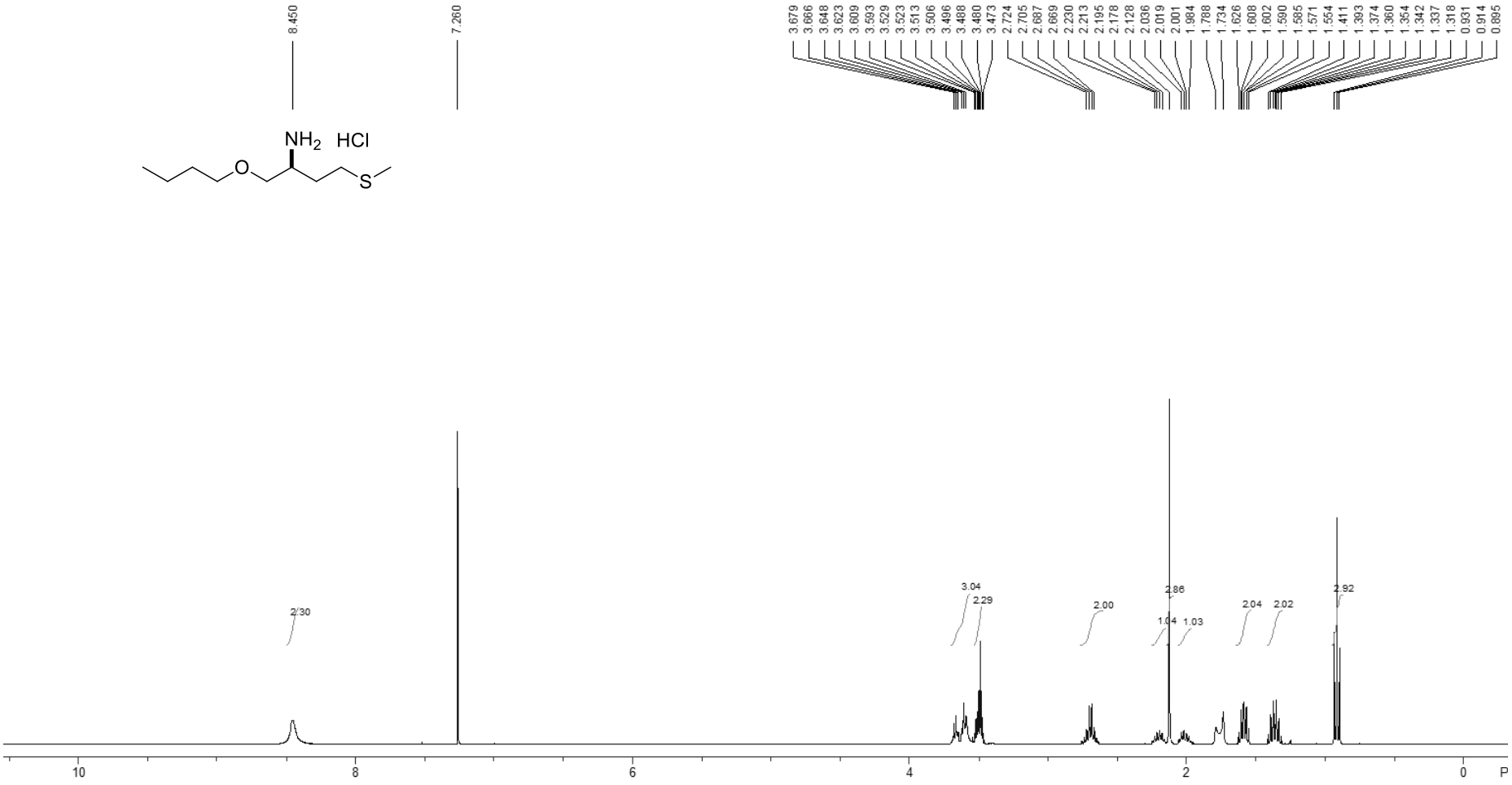

Figure S24. ^{1}H NMR (400 MHz, $CDCl_3$) of **10**.

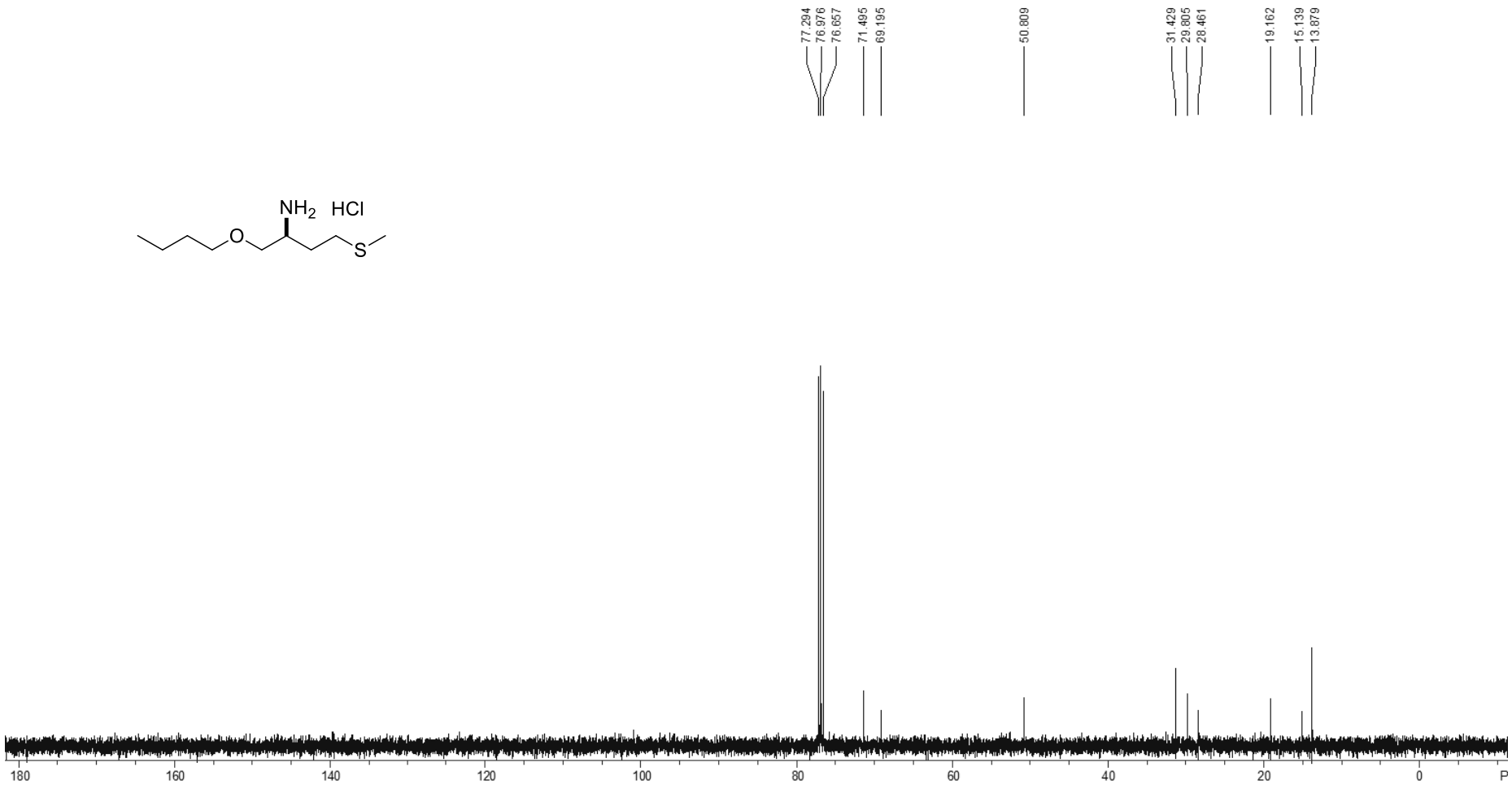

Figure S25. ^{13}C NMR (100 MHz, $CDCl_3$) of **10**.

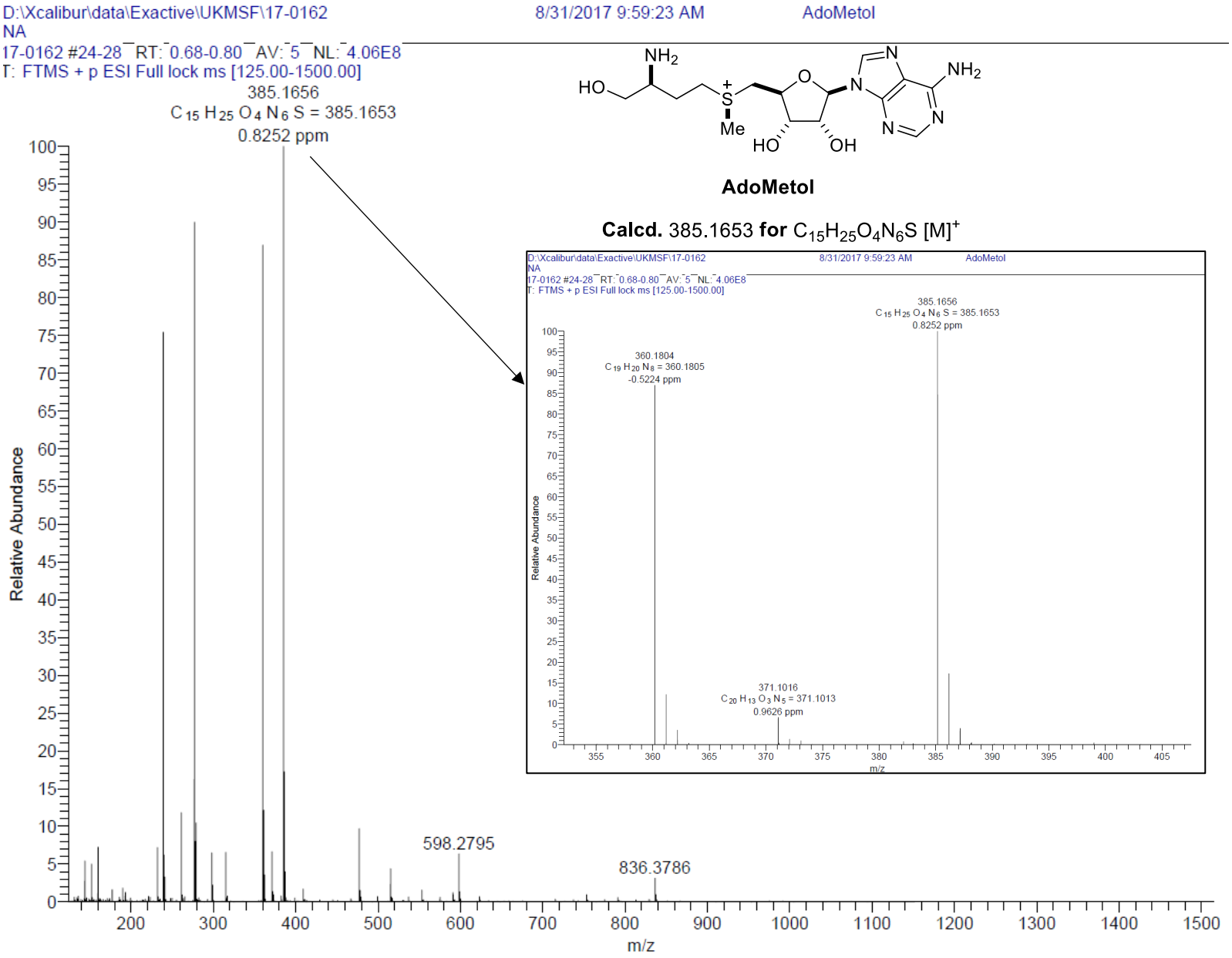

Figure S26. HRMS of **AdoMetol**.

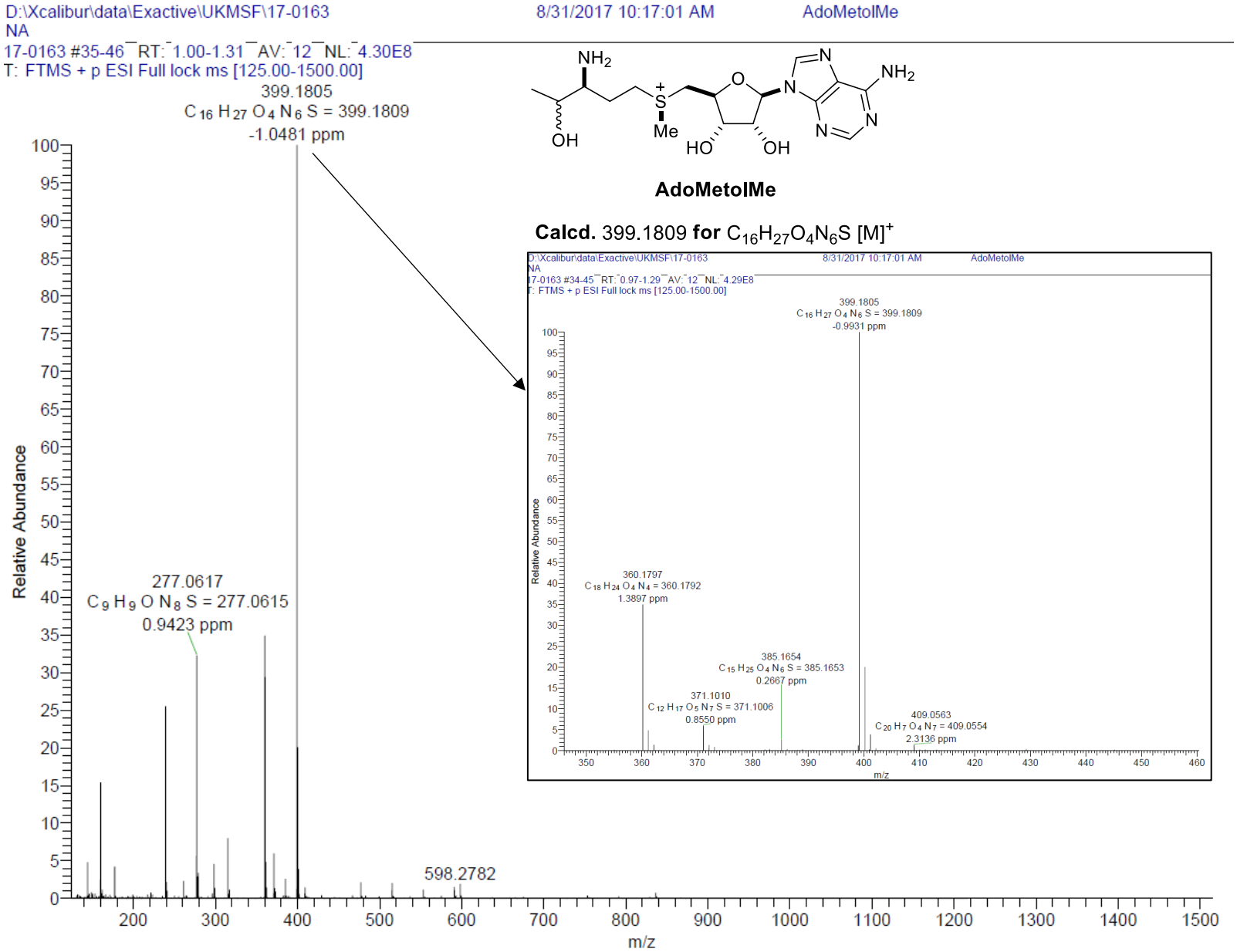

Figure S27. HRMS of **AdoMetolMe**.